MASARYKOVA UNIVERZITA
PŘÍRODOVĚDECKÁ FAKULTA
ÚSTAV TEORETICKE FYZIKY A ASTROFYZIKY

Diplomová práce

BRNO 2015   VLASTA GLIŠIĆ

MASARYKOVA UNIVERZITA
PŘÍRODOVĚDECKÁ FAKULTA
ÚSTAV TEORETICKE FYZIKY A ASTROFYZIKY

Parametry větru horkych hmotnych hvězd z ultrafialove spektroskopie

Diplomová práce

Vlasta Glišić

Vedoucí práce: Mgr. Brankica Šurlan, Ph.D.   Brno 2015

Bibliografický záznam

Autor: Bc. Vlasta Glišić
Přírodovědecká fakulta, Masarykova univerzita
Ústav teoreticke fyziky a astrofyziky

Název práce: Parametry větru horkych hmotnych hvězd z ultrafialove spektroskopie

Studijní program: Teoreticka fyzika a Astrofyzika

Studijní obor: Astrofyzika

Vedoucí práce: Mgr. Brankica Šurlan, Ph.D.

Akademický rok: 2014/2015

Počet stran: ix + 63

Klíčová slova: horke hvězdy, hvězdny vítr, modelování, shlukování, parametry větru

Bibliographic Entry

Abstrakt

Horké hmotné hvězdy a jejich větry hrají klíčovou roli v chemické evoluci a dynamice evoluce galaxií a mají silný vliv na mezihvězdné prostředí. Přesná stanovení základních parametrů těchto hvězd jsou relevantní pro pochopení jejich vývoje a vývoje jejich hostitelských galaxií. V této práci jsme odvodili hvězdné parametry a parametry větru dvou galaktickych hvězd typu O: HD 34656 a HD 188001. Bylo analyzováno daleké ultrafialové a blízké ultrafialové spektrum pořízené družicemi FUSE a IUE a optické spektrum získané z dalekohledu Perek v Ondřejově. Spektra byla modelována Potsdam Wolf-Rayet (PoWR) kódem modelu atmosféry a v souladu s nimi byly stanoveny hvězdné a větrné parametry. Poté byly, pomocí 3D Monte Carlo kódu přenosu záření pro nehomogenní vítr, určeny parametry shlukování.

Abstract

Hot massive stars and their winds play a crucial role in the chemical and dynamical evolution of galaxies and have strong impacts on interstellar medium. Accurate determination of fundamental parameters of these stars are relevant for understanding their evolution and evolution of their host galaxies. In the present work we derived stellar and wind parameters of two Galactic O-type stars: HD 34656 and HD 188001. Far-ultraviolet and near-ultraviolet spectra taken with FUSE and IUE staelites and optical spectra obtained from Perek telescope in Ondrejov, were analyzed. The spectra were modelled with Potsdam Wolf-Rayet (PoWR) model atmosphere code and stellar and wind parameters where consistently determined. After those values were established, the 3D Monte Carlo Radiative Transfer code for inhomogeneous wind was used and clumping parameters were estimated.

Masarykova univerzita

Přírodovědecká fakulta

ZADÁNÍ DIPLOMOVÉ PRÁCE

Student   : **Bc. Vlasta Glišić, učo <u>426947</u>**

Studijní program : **Fyzika**

Studijní obor   : **Teoretická fyzika a astrofyzika**

Ředitel Ústavu teoretické fyziky a astrofyziky PřF MU Vám ve smyslu Studijního a zkušebního řádu MU určuje diplomovou práci s tématem:

<u>Parametry větrů horkých hmotných hvězd z ultrafialové spektrokopie</u>

Wind parameters of hot massive stars from ultraviolet spectroscopy

Zásady pro vypracování: Ultrafialová spektroskopie umožňuje přístup k základním diagnostickým čarám větrů horkých hvězd. Cílem diplomové práce je určit parametry větrů vybraných hvězd. Budou použita archivní ultrafialová spektra z družic IUE a FUSE spolu s optickými spektry z Perkova dalekohledu v Ondřejově. Spektra budou analyzována pomocí NLTE modelů hvězdných větrů. Práce bude vypracována v angličtině.
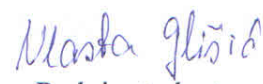
Literatura:

- LAMERS, Henny J. G. L. M. a Joseph P. CASSINELLI. *Introduction to stellar winds.* Cambridge: Cambridge University Press, 1999. xiv, 438 s. ISBN 0-521-59565-7.

- PULS, J, J S VINK a F NAJARRO. Mass loss from hot massive stars. *The Astronomy and Astrophysics Review*, 2008, roč. 16, s. 209-325.

- FULLERTON, Alex W. *Observations of Hot-Star Winds.* : Springer Verlag, 1997. s. 187-237.

Jazyk závěrečné práce   : anglický

Vedoucí diplomové práce   : Mgr. Brankica Šurlan, Ph.D.

Datum zadání diplomové práce   : leden 2014

Datum odevzdání diplomové práce : dle harmonogramu ak. roku 2014/2015

V Brně   leden 2014   Rikard von Unge

                                                    ředitel ÚTFA

Zadání diplomové práce převzal dne: Podpis studenta

Poděkování

I would like to say big "Thank You" to my supervisor Brankica Šurlan for all constructive suggestions and patience she showed me during writing this thesis. Also special thanks goes to prof. Wolf-Rainer Hamman for his invaluable suggestions and great knowledge he passed to me during my visits to Potsdam and to Tomer Shenar, Reiner Heinich, Helge Todt and Andreas Sander for all patience asnwering all my questions and giving insights into code tips and tricks. Last, but not least, I want to thank my family and friends for support they gave me during all my studies.

Prohlášení

I declare that I wrote my thesis independently and exclusively with the use of references cited. I agree to lending and publishing of the thesis.

Brno 13. května 2015

....
Vlasta Glišić

Contents

List of Tables

List of Figures

Chapter 1

Introduction

Massive stars are usually classified as stars with masses higher than $\approx 8M_\odot$. Hot stars, with their effective temperatures higher than $\approx 25\ 000$ K on main sequence and luminosities higher than $L \approx 10^2 L_\odot$, represent important and intriguing objects in our Universe. Strong ionizing fluxes, which create H II regions, are observed as a direct consequence of their high temperatures. These stars live short lives ~ 5 - 20 Myr on the main sequence. Due to their high masses these objects end their lives as a core collapse supernovae, causing "feedback" to interstellar medium (ISM). Gamma ray bursts are an alternative way in which these stars can end their lives (Kudritzki and Urbaneja, 2006; Puls et al., 2008). They produce, unlike low mass stars, in their core many elements heavier than oxygen and are major producers of so-called α elements[1]. All hot stars are characterized by high radiation energy densities and expanding atmospheres i.e., stellar winds. More about basic properties of hot massive stars and their values see Crowther (2004); Martins (2010, 2014)

Stellar wind is described by mass-loss rate and terminal velocity. By this stellar wind, star enriches the ISM with products of its core burning.At the beginning of research the wind of hot massive stars were thought to be stationary, smooth and spherically-symmetric with a monotonic velocity field. In the later phases of research some observational indications, including non-thermal radio emission (Abbott et al., 1981), black absorption troughs (Lucy, 1982) and soft X-rays emission (Harnden et al., 1979; Seward et al., 1979) suggested that these winds are in fact inhomogeneous. In addition to those observational evidences of large-scale structures in the wind, there were also observational evidences that the wind consists of a widespread large number of stochastic structures on small scales, so-called *clumps*.

Mass-loss influences the evolution of stars of all masses, but its the major influence is on the evolution of hot stars, due to their high luminosities, which can have extremely strong stellar winds (Vink, 2008). During the time the star spends on the main sequence it can lose significant fraction of its initial mass which, consequently, imposes different conditions of star's further evolution affecting surface abundances and luminosity of the star.

Hot massive stars are located at the upper left corner of Hertzsprung-Russell dia-

---

[1] α elements are called that way since their isotopes represent the integer multiple of 4, or in other words mass of the He core which itself is called α particle.

Figure 1.1: Hertzprung-Russell diagram, adopted from http://www.wwu.edu/skywise/a101_hrdiagram.html on 25.04.2015

gram, corresponding to spectral types O and early B on the main sequence and their later evolutionary stages include supergiants and Wolf-Rayet (WR) stars (Crowther, 2004; Martins, 2014).

Massive stars are often found in star forming regions which are heavily obscured by interstellar dust (Kudritzki and Urbaneja, 2006) and are the only stellar objects observed in high redshift galaxies (Crowther, 2004). These stars, even though they comprise for just a tiny fraction of total number of stars in galaxy, are vital for our understanding of the galaxy itself. On the local level, they are responsible for existence of H II regions and are believed to trigger star formation. If we now look at the bigger picture, they influence chemical and dynamical evolution of the global ISM of their host galaxies (Kudritzki and Puls, 2000). Reliable estimates of their basic stellar parameter are essential in order to understand these intriguing objects.

Observed spectra of those objects contain information about matter stellar radiation passes through. In order to decode those information and deduce stellar and wind parameters we need to compute synthetic spectra which are obtained by solving the radiative transfer equation. To obtain a consistent solution of the radiative transfer equation, efficient numerical tools are needed.

Most important of such tools are *unified model atmospheres*. These models are stationary, in NLTE and radiative equilibrium, spherically extended and produce the entire subsonic and supersonic atmosphere structure of radiation driven winds, taking density and velocity stratification from hydrodynamics or adopting a smooth transition between outer and inner structure of the wind. Nowadays, such models are used to calculate energy distribution simultaneously with photospheric and wind lines and their main advantage is that they can treat a multitude of so-called mixed cases where photospheric line is "contaminated" by wind (Kudritzki and Puls, 2000). Also, they explicitly allow for line-blanketing effect to be included. The calculation of such models, that include spherical-symmetry and full line blanketing effects, is extremely

time consuming (Hillier et al., 2003). However, the fact of long computational time is awarded by more reliable estimates of wind parameters in particular.

This thesis focuses on using one of those unified model atmospheres in order to derive stellar and wind parameters of selected stars. In the first step, observed spectra in optical and UV region are obtained. Then, initial values of stellar and wind parameters are looked up in literature and are given as an input into the PoWR code. This code calculates synthetic spectrum which is compared to the observed one and then certain stellar or wind parameters are changed in order to achieve satisfying fit between the two spectra. After satisfying fit was obtained, mass-loss rate is given as an input to the 3-D Monte Carlo Radiative Transfer code for inhomogeneous winds in order to derive clumping parameters of the wind. This step is done in order to solve discrepancies in the values of mass-loss rate obtained from optical (H_α) and UV (P V) diagnostics.

In order to easily follow this thesis in following chapter winds of hot massive stars are discussed, their characteristics, driving mechanism, parameters and spectral diagnostics. Chapter 3 represents the basic theory of stellar atmosphere and brief description of 2 numerical codes used in the thesis. Studied stars, their properties and observations are presented in chapter 4, while the results of spectroscopic modeling are given in chapter 5. Finally, chapter 6 represents the summary of this work.

Chapter 2

Winds of hot massive stars

All hot massive stars exhibit stellar wind. It represents the continuous outflow of particles from their surface. In all hot stars these winds are driven by radiation. The origin of this wind lays in high luminosity of massive stars. Dominant spectroscopic signature of stellar winds are line profiles which are formed in rapidly expanding part of the wind. Wind momenta and energies contribute to dynamics of ISM in galaxies or surrounding gaseous nebulae. These winds are fundamentally important since their energy and momentum input into ISM is significant creating circumstellar shells, wind bubbles and initiating star formation. Stellar evolution is also affected by the presence of a stellar wind since it modifies surface abundances, stellar luminosities and finally stellar evolution itself.

Nowadays,wind lines can be easily identified form medium resolutions spectra of hot stars out to distances of 20 Mpc or in integrated spectra of starburst regions in galaxies out to redshifts $z \sim 4$ using new ground based facilities, with telescopes of 10-m class. In search for information about young stellar populations, chemical compositions, extragalactic distances and galactic evolutions stellar winds can provide us with crucial answers (Kudritzki and Puls, 2000). From all of this we can see that stellar winds have important role in understanding massive stars and consequently their host galaxies.

2.1 Driving mechanism of hot massive stars winds

Atmospheres of hot massive stars are not in radiative equilibrium (i.e., radiation overcomes gravity) and due to that it comes to the outflow of the gas from the stellar surface. Winds of luminous stars are driven by absorption of photospheric photons in spectral lines and they are called **line driven winds** (Lamers and Cassinelli, 1999). As is know from quantum mechanics, photon can be absorbed only if its energy is equal to the difference of the energy between lower and higher energy level, i.e., if its energy is equal to an energy needed to excite the atom (or ion) to higher energy level $h\nu = E_2 - E_1$. Here ν represents the frequency of absorbed photon, h is the Planck constant,[1] E_2 is the excited energy level and E_1 is the ground energy level. In this excited state ion can stay for a very short amount of time, after which it

---

[1]Value of Planck constant is $h = 6.625 \cdot 10^{-34} Js$

returns to lower energy state and photon is being re-emitted. This process is called *line scattering* and if the line transition is from the ground state, then that specific line is called *resonance line* and thus the processes is called *resonance line scattering*. This process is shown in the figure 2.1. Most P Cygni line profiles are formed from resonance line scattering. The radiative acceleration caused by spectral lines drives the wind of many different star types: giants and supergiants of types O, B and A; central stars of planetary nebulae and white dwarfs.

Apart from the process of line scattering, Coulomb collisions are necessary to drive the wind of hot stars. As it turns out, H and He are inefficient in accelerating the wind and represent passive components. Since the wind of hot star is ionized, the most efficient way of transferring momentum from heavier elements (metals) to passive components are Coulomb collisions (Krtička and Kubát, 2007). Because H and He have few lines in the relevant spectral range in which hot stars emit majority of their radiation (UV range), lines of metals are responsible for line driving.

Pioneers in the field of radiation driven wind theory were Lucy and Solomon (1970) (who suggested that absorption in UV resonance lines can resist stellar gravity and set up a continuous mass flow) and Castor et al. (1975) who made significant progress in hot star wind theory. These authors solved hydrodynamic equations, which treated wind as a single fluid, assuming that wind is driven by radiation pressure. They constructed the wind model based on assumptions that wind is spherically-symmetric, stationary, homogeneous and that there are no magnetic fields in it. This model is known as *CAK wind model* or *standard wind model*.

Physical processes in line driven winds   Properties of stellar winds depend on number of metal lines available to absorb the photon and their ability to absorb it. When the photon is absorbed and re-emitted it transfers its momentum and energy to the absorbing atom. The radiative acceleration in the winds of hot stars is provided mainly by absorption and re-emission of UV photons in the resonance lines of ions of abundant elements such as C, N and O and Fe-group elements in the Lyman continuum. In order to accelerate the wind to the terminal velocity $v = 2000$ km s^{-1} it is needed to have roughly 10^{11} absorptions per absorbing ion (Lamers and Cassinelli, 1999). In order to provide such acceleration the ions must absorb 10^7 photons per second. This implies that only transitions to levels with short lifetimes ($\approx 10^{-7}$ s) will contribute effectively to radiative accelerations. Levels with larger lifetimes can also contribute to this acceleration if their number is sufficiently large. The radiation provides the wind with kinetic energy, the potential energy to lift the gas out of the potential well of the star and the thermal energy (Lamers and Cassinelli (1999), p. 188).

Lines that drive the winds   At the highest temperatures $T_{\text{eff}} \approx 50$ kK the largest contribution to the wind comes from the lines of Ne to Ca (mainly Si, S, P). At the temperature range 25 kK $\lesssim T_{\text{eff}} \lesssim 40$ kK dominant contribution is by C, N and O and especially N IV and O IV. Between 6 kK $\lesssim T_{\text{eff}} \lesssim 25$ kK dominant contribution is provided by the elements of Fe-group (Lamers and Cassinelli (1999), p.219-221). We can also say that CNO elements are principal line drivers in supersonic (outer)

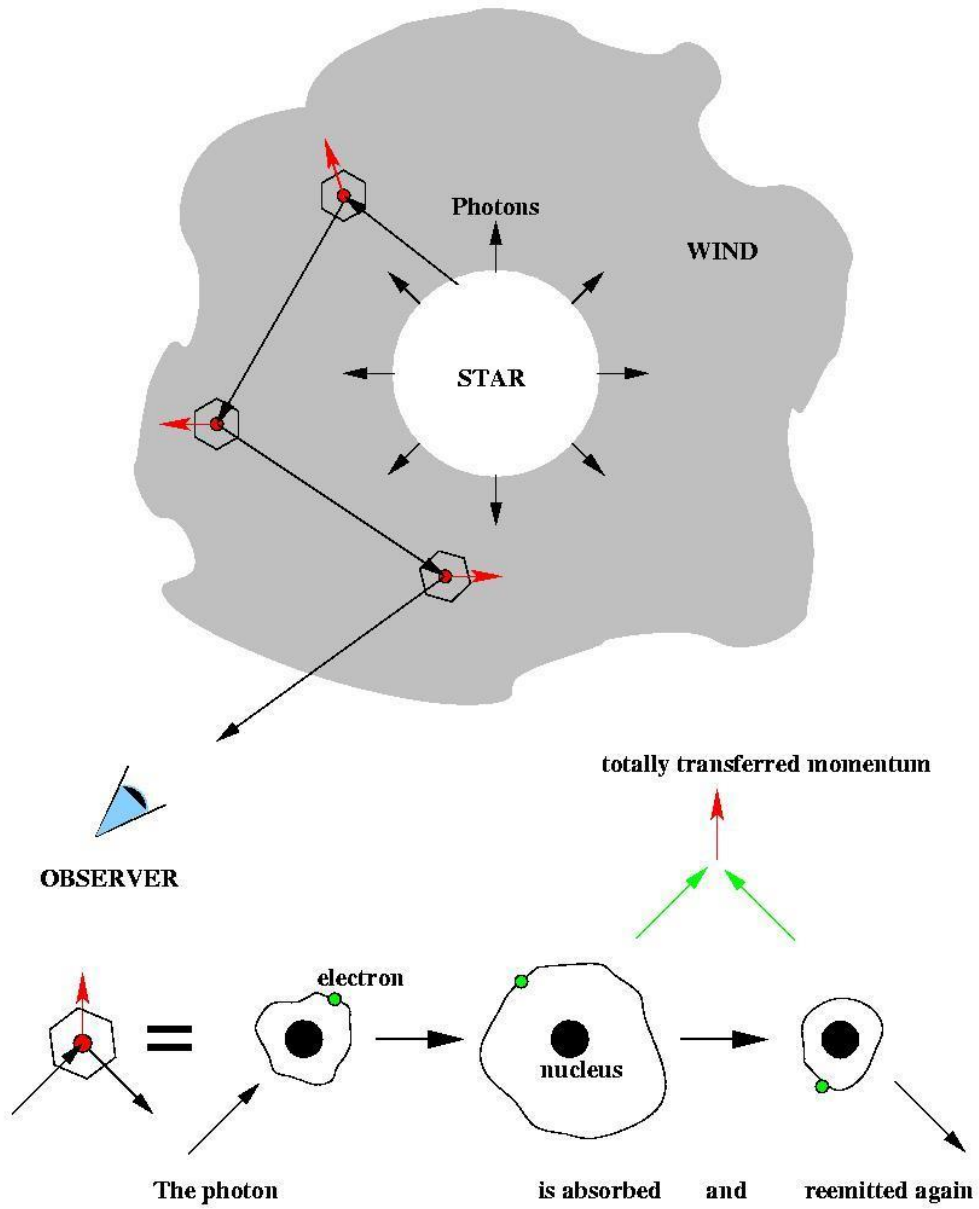# The principle of radiatively driven winds

Figure 2.1: Principle of radiative line driving in stellar winds. Adapted from home-page of Joachim Puls on 2.3.2015

part of the wind and that the elements of Fe-group are dominant line drivers in subsonic (inner) part of the wind (Crowther, 2004).

2.2   Wind parameters

Two main parameters used to describe the wind are *mass-loss* $(\dot{M})$ and *terminal velocity* (v_∞). Mass-loss rate represents the measure of mass the star loses in certain amount of time. It is usually expressed in units of solar mass per year $(M_\odot \ yr^{-1})$. Mass-loss rate for massive stars is as high as $\dot{M} \approx 10^{-5} \ M_\odot \ yr^{-1}$(Crowther, 2004; Hillier, 2010). Terminal velocity is the maximum velocity of the wind, achieved far from the stellar surface, assumed $r \geq 10 \ R_*$. The range in velocities is considerable from $v_\infty = 3500 \mathrm{km\,s}^{-1}$ in the earliest O-type stars to $v_\infty = 100 \ \mathrm{km\,s}^{-1}$ for some AB supergiants (Crowther, 2004).

Determination of these parameters from observations is not an easy task to complete, especially since they are not directly observable. Due to this, we have to use atmospheric models in order to estimate those parameters. Models used include hydrodynamic effects of the wind which are basis for radiative transfer calculations to be compared with observations. The easiest approach is to use so-called standard wind model assumptions of stationary spherically-symmetric smooth stellar wind. In this model, mass-loss rate is derived via continuity equation as:

$$\dot{M} = 4\pi R_*^2 \rho(r) v(r) \tag{2.1}$$

where R_* is the stellar radius, $\rho(r)$ and $v(r)$ are density and velocity distributions, respectively (Kudritzki and Puls, 2000). In the standard wind model velocity field in the supersonic region has the form:

$$v(r) = v_\infty \left(1 - b\frac{R_*}{R}\right)^\beta, \ b = 1 - \left(\frac{v(R_*)}{v_\infty}\right)^{1/\beta} \tag{2.2}$$

where b is a constant that fixes the velocity at the inner boundary of the wind to the prespecified value of $v(R_*)$ which is usually of the order of the sound speed which has little influence on the computed spectrum. This type of dependence for velocity was derived by Milne (1926). In the formula 2.2 β describes the steepness of the velocity law, that is how fast the wind velocity is approaching v_∞. Typical value of the β parameters for O-type stars is $\beta \sim 0.8 - 1.5$ (Crowther, 2004).

In this wind model, additional information is needed in order to calculate synthetic spectrum including the radiation field from the photosphere, which can be obtained from photospheric model, and electron temperature which is assumed to be equal or lower than the effective temperature of the star (Kudritzki and Puls, 2000). In calculation of the synthetic spectrum, $\dot{M}$, v_∞ and β are treated as "fit parameters" which are determined from the spectrum. These parameters are changed until satisfactory fit of the synthetic to observed spectrum is achieved.

Reliability of the estimated global wind parameters depend on the model used and also on part of the spectrum used. Another important characteristics that has

to be taken into account when estimating the global wind parameters, and especially $\dot{M}$ is the inhomogeneity of the wind and how the selected model treats it.

Alternative way in how to derive global wind parameters is from wind hydrodynamics by dolving the continuity equation and momentum equation. These equations can be written, in approximation that stellar wind is treated as a single-fluid, neglecting viscosity and forces due to electric and magnetic fields:

$$\frac{\partial \rho}{\partial t} + \nabla \cdot (\rho \mathbf{v}) = 0 \tag{2.3}$$

$$\frac{\partial v}{\partial t} + (\mathbf{v} \cdot \nabla)\mathbf{v} = -\frac{1}{\rho}\nabla p + \mathbf{g}_{\mathrm{ex}} \tag{2.4}$$

where $\mathbf{v}$, ρ is the mass density, p is the pressure of gas and $\mathbf{g}_{\mathrm{ex}}$ is the vector of external acceleration, which includes gravitation and radiation forces. However, model atmosphere used in this thesis do not solve these equations, velocity field is assumed to be approximater by equation 2.2 and density is calculated from 2.1.

2.3   Clumping in the wind

In the very beginning of the research in the field of winds of hot stars it was assumed that the wind is stationary, spherically symmetric and *homogeneous* (CAK theory). However, theoretical evidences (eg., Owocki et al. (1988) or Feldmeier (1995)) were that the wind is actually time-dependent and inhomogeneous. Theoretical basis four our understanding and interpretation of clumping represents the so-called "line-driven instability"[2] and it was shown that its growth leads to compression of wind material into dense and spatially narrow clumps which are separated by area of lower densities (Sundquist et al., 2011). First observational evidence for those wind inhomogeneities, "clumping", for O-type stars came at the end of 20th century (Eversberg et al., 1998) and recently by Lépine and Moffat (2008) where they reported on observing emission substructures in the radiation driven winds of hot stars in different evolutionary stages. Clumping manifests itself through small-scale fluctuations in emission profiles (Hillier, 2010). There are suggestions that clumping begins at low velocities and is less in the radio-emitting region (Crowther, 2004). Main influence of clumping is that its presence leads to increase of electron density inside the clumps, which further results in higher recombination rates and the wind becomes less ionized which in the end leads to increase in the wind velocity (Krtička et al., 2008). Clumping can be treated either in microclumping or macroclumping approach.

In PoWR (and other state-of-the-art model atmospheres) clumping is taken into account in first approximation (microclumping) with the main assumption that the clumps are smaller than the photon's mean free path for all frequencies, i.e., they are *optically thin*. Additional assumption is that the density inside the clumps is uniform and enhanced by factor D compared to a smooth model with same mass-loss rate.

---

[2]It is an intrinsic effect which shows that line-driven winds should become unstable around certain scale called Sobolev length.

Interclump medium is assumed to be void and therefore the volume filling factor of the clumps is expressed as $f_V = D^{-1}$ (Hamann et al., 2008). Wind emission lines, including also the H_α line, are recombination lines and therefore are dependent on density squared. When mass-loss rate is estimated from this line, using model that accounts for microclumping, the value derived will be lower by a factor $\sqrt{D}$ than from a smooth-wind model (Hamann et al., 2008; Oskinova et al., 2007). In PoWR typical clumping factor is between 4 and 10, which gives good results for WR stars, but unfortunately is not applicable for O-type stars since their spectra do not show suitable emission wings (Hamann et al., 2008).

Only justification for usage of microclumping approach was simplicity. Oskinova et al. (2007) relaxed the microclumping approximation in favor of a generalized treatment that allows the possibility of clumps being optically thick at some frequencies which they refer to as *macroclumping* approach. They are producing macroclumps by merging few microclumps without changing the matter density and allow for the size of the macroclump to exceed the photon's mean free path at frequencies with large atomic cross section. Same authors are actually inferring that the clump is optically thick in the cores of strong spectral lines, while at all other frequencies it remains optically thin. These optically thick clumps lead to a local shielding of opacity which in turns allows for increased escape of radiation through porous channels between the clumps (Sundquist et al., 2011). This effect, sometimes referred to as porosity, leads to increase of the wind ionization, which consequently leads to decrease of radiative force and in the end the mass-loss rate may decrease (Krtička et al., 2008). Another effect of the macroclumping approach is velocity porosity or sometimes referred to as vorosity. It is an effect that the line photon can pass through porous channels in velocity space, without interacting with clumps (Owocki, 2008).

Selection of the approach in which the clumping is treated has strong influence on synthetic spectra and consequently on estimates of wind parameters.

2.4   Spectroscopic diagnostics

Diagnostic methods of stellar winds represent important tools for the determination of stellar and wind parameters from observed spectra. Wind line can be distinguished from photospheric line because it appears in absorption, emission or as a P-Cygni profile (combination of absorption and emission).

Typical wind lines are P Cygni line profiles. This profile arises in the stellar wind, and is composed of blue absorption and red emission part. Formation of this profile is intuitively easily understood. In the figure 2.2 we see 4 regions observer can distinguish. The "STAR", the "F" region containing radiation coming towards the observer, the "O" region containing radiation going away from the observer (it cannot be detected) and the region "H" or so-called halo surrounding the star. The star itself emits continuum radiation. Region "F" then scatters radiation coming from the star which would reach the observer in ideal case without stellar wind. In the realistic case, with stellar wind, part of the radiation coming from the star is scattered away from the line of sight of the observer and that produces blue shifted absorption part of the P-Cygni profile. Emission part, with red shift, comes from

the scattering of the radiation in the halo of the star, that normally would not be registered by the observer, to the "F" region (Lamers and Cassinelli, 1999). Both of these effects combined together (simple addition) give rise to the famous P-Cygni profile.
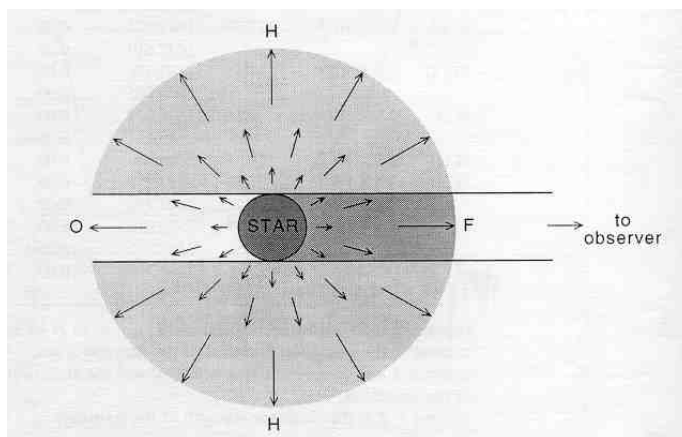

Figure 2.2: Geometry of stellar wind, adapted from Lamers and Cassinelli (1999)

Typical examples for P-Cygni profile represent UV resonance transitions connected to the ground level (Kudritzki and Puls, 2000). Lines of most importance for study of stellar wind with this profile are located in the UV part of the spectrum.

Spectroscopic analysis gives us possibility to maximize the amount of information we can extract from the observation. By the means of spectroscopy we can obtain information about temperature, luminosity, surface gravity and surface abundances. In this thesis I will focus of optical and UV spectroscopic diagnostics, but they are in no way the only diagnostics one can use. Infrared (IR), radio or X-ray spectra provide also good diagnostic tools for investigating crucial stellar and wind parameters, but they are beyond the scope of this thesis.

2.4.1 Optical diagnostics

Lines found in the optical part of the spectrum can be used to determine effective temperature, surface gravity or surface abundances, but also wind parameters such as mass-loss rate, terminal velocity or β exponent (see equations 2.1 and 2.2).

Effective temperature   One of the most used methods in deriving effective temperature is ratio of He I λ4471 to He II λ4542 equivalent widths since they are the strongest photospheric lines (Bouret et al., 2012; Kudritzki and Puls, 2000; Martins et al., 2015). In general, He lines represent good diagnostic tool for constraining the effective temperature, with exception of He I λ5876 to He II λ4686 since these two lines are affected by the stellar wind (Martins et al., 2015). One also has to bear in mind that, if the temperature is lower than 27 kK then the He II is not a dominant ionization degree and thus He II lines cannot be used as a temperature diagnostics
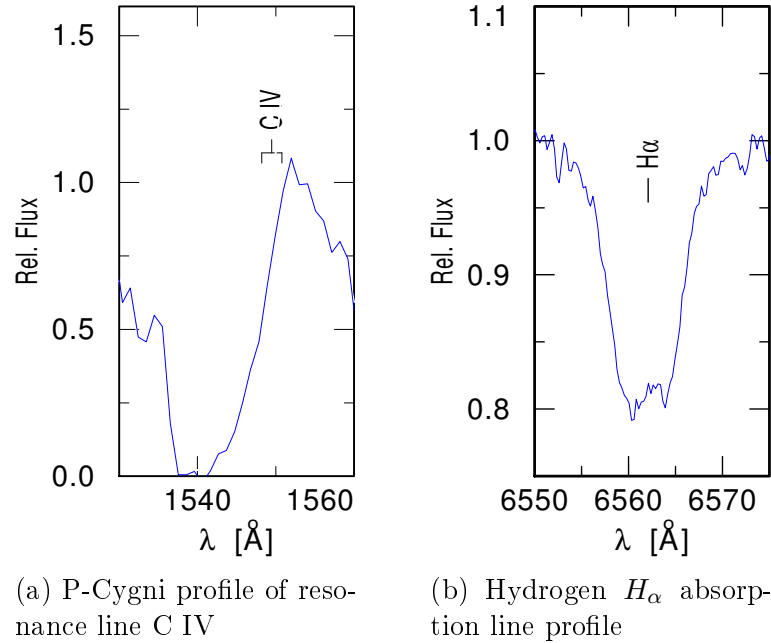
(a) P-Cygni profile of reso-
nance line C IV

(b) Hydrogen H_α absorp-
tion line profile

Figure 2.3: Example of absorption and P-Cygni line profile of star HD 34656. Ab-
sorption profile was obtained by 2-m telescope at Ondřejov observatory, while the
P-Cygni profile was taken by IUE satellite.

in this case and other lines, such as Si lines are used (Martins, 2010). Typical uncer-
tainties in deriving the value of effective temperature is up to 5% depending on the
quality of observation (Martins, 2010). Determination of the effective temperature
is dependent on assumptions that we insert into our model and the accuracy with
which the surface gravity and surface abundance are determined (Crowther, 2004).

Surface gravity   Surface gravity is one of the stellar parameters that is classically
determined from optical diagnostics. Surface gravity is expressed in logarithmic
value as $\log g$. Primary diagnostic for surface gravity represent the Stark-broadening
wings od Balmer lines, except H_α and H_β since they are "contaminated" by the
wind (Bouret et al., 2012; Martins, 2010). The wings of these lines are broadened by
collisional processes and are stronger in denser atmospheres (meaning higher surface
gravity which causes larger pressure and more collisions). These Balmer lines need
to be in absorption and/or their wings must not be contaminated by wind emission
in order to be suitable as surface gravity diagnostics. Luckily, they are usually strong
and well resolved (Martins, 2010).

Surface abundances   Determination of surface abundance is done using photo-
spheric lines. Optical studies of O-type stars allow us to determine abundances of
C, N, O, Si and Mg (Martins, 2010). The method consists of comparing synthetic
and observed spectra for given set of abundances and then changing the abundances
until the satisfactory fit is achieved. Main lines used are:
-carbon: C II $\lambda4267$, C II $\lambda\lambda6578 - 82$/ C III $\lambda\lambda4647 - 50$, C III $\lambda5696$/C IV

$\lambda\lambda 5801 - 12$;

-nitrogen: N II $\lambda 3995$/N III $\lambda\lambda 4510 - 15$/N IV $\lambda 4058$, N IV $\lambda 5200$/N V $\lambda\lambda 4605 - 20$;

-oxygen: O II $\lambda 4075$, O II $\lambda 4132$, O II $\lambda 4661$/O III $\lambda 5592$;

-silicon: Si II $\lambda\lambda 4124 - 31$/Si III $\lambda\lambda\lambda 4552 - 67 - 74$, Si III $\lambda 5738$/Si IV $\lambda 4089$, Si IV $\lambda 4116$;

-magnesium: Mg II $\lambda 4481$ (Martins, 2010).

Another important parameter that is needed in order to derive correctly the surface abundances for O-type stars is microturbulent velocity. It can be constrained from few metallic lines and its determination is usually done simultaneously with surface abundances (Martins, 2010).

Mass-loss rate   Optical emission lines, mainly H_α are used to constrain value of mass-loss rate $\dot{M}$ and also He II $\lambda 4686$ is sensitive to the change of mass-loss rate (Bouret et al., 2012; Martins, 2010). If the star possesses strong stellar wind then the profile of H_α is in emission. Since it is recombination line, it does not depend on density as eg. P V but on the density square and the emission observed in H_α decreases quickly with density leading to weaker winds. This line can even turn into a pure photospheric line if the mass-loss rate is $\sim 10^{-8} M_\odot \ yr^{-1}$ and therefore cannot be used to derive $\dot{M}$ (Martins, 2010). Another problem that can occur with using H_α as a mass-loss diagnostic, especially in O-type stars, is that it can blend with He $\lambda 6560$ or other problems such as nebular contamination from H II regions and broadening of the central emission component by stellar rotation (Crowther, 2004). Its advantage, however, is that it is less sensitive to ionization fraction than P V, since H is almost completely ionized in atmospheres of hot stars (Martins, 2010).

Terminal velocity   The terminal velocity can be defined in two ways, either as a velocity leading to the absorption up to the point where certain line reaches the continuum or as a velocity that produces the blue complete absorption. If the wind is strong enough we will observe P-Cygni profile in some lines. For purpose of determining the terminal velocity lines of Balmer series (H_α, H_β, H_γ, H_δ) and some He I lines, such as He I $\lambda 4417$ can be used (Martins, 2010). If the line has P-Cygni profile then from fitting the blue absorption edge we constrain the value of terminal velocity. However if the line has pure emission profile then the line widht is usually related to terminal velocity. Both of the methods provide indirect measure of terminal velocity of the wind (Martins, 2010).

β-velocity field exponent   In order to derive the velocity field of the wind, β law approximation is used (see equation 2.2). Exponent β used in that law can be determined from shape of certain optical lines. Good diagnostic for its value are lines H_α and He II $\lambda 4686$ since their shape is sensitive to changes in β. However, we must know that these lines are also used as a diagnostics for mass-loss rate in optical region so their intensity will correspond to changes in mass-loss rate while shape of the lines corresponds to the value of β exponent (Bouret et al., 2012). Of these two lines, better diagnostics gives H_α line since it is formed in the outer photosphere and lower or intermediate wind (Lefever et al., 2007).

Clumping parameters As is already said, winds of hot stars are not homogeneous. To find the degree of clumping in strong stellar wind it is used the electron scattering wings of emission lines, with classical line diagnostics being He II $\lambda4686$, He II $\lambda5412$ and H_β. The main effect clumping has on lines is that it changes the shape of wind lines (for a given atmospheric structure) and ionization structure is modified due to increased density in clumps (Martins, 2010).

2.4.2 Ultraviolet diagnostic

For O-type stars is shown that they experience maximum of its radiation in UV part of the spectrum. Also determination of wind parameters is dependent on certain lines that are found in UV part of spectrum (such as C IV $\lambda\lambda1548-50$, Si IV $\lambda\lambda1393-1403$ or P V$\lambda\lambda1118-28$). Since Earth's atmosphere is blocking those wavelengths the only way to observe UV spectra of a stellar object is to observe the object outside the atmosphere. The most important rockets to observe in UV were International Ultraviolet Explorer (IUE) and The Far Ultraviolet Spectroscopic Explorer (FUSE) which observed certain star in near UV (NUV) and far UV (FUV), respectively. UV spectra and UV diagnostics are important since they contain saturated P-Cygni profiles which are useful for various wind diagnostics.
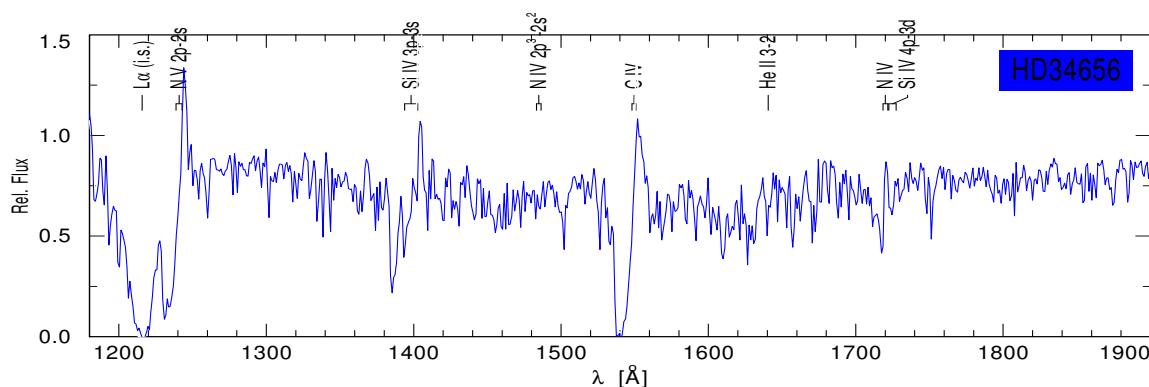
Figure 2.4: Example of NUV spectrum of star HD 34656, taken by IUE satellite.

Effective temperature Determination of effective temperature based just on UV spectra is difficult. For example, Fe ionization balance can be used to estimate effective temperature. Line forests from Fe IV are observed in wavelength region $\lambda\lambda1600-30$, Fe V in wavelength region $\lambda\lambda1360-80$ or Fe VI in wavelenght region $\lambda\lambda1260-1290$ (Martins, 2010) Ionization ratios of Fe IV to Fe V and Fe V to Fe VI provide a sensitive temperature diagnostic (Bouret et al., 2012).

Surface abundances In the UV region CNO and Si lines are usually wind lines and are used for deriving terminal velocity and mass-loss rate. In this region, however, there are several Fe-line forests (upper paragraph) that can be used for deriving

Fe abundance. If relative strength of these lines gives value of T_{eff} then their absolute strength is an indicator of the Fe composition (Martins, 2010).

Terminal velocity   For deriving the terminal velocity we are using saturated lines (i.e., lines that have steep absorption edge and reach the continuum). Velocity at which one saturated line reaches the continuum is $v_{edge} \approx -(v_\infty + 2v_{turb})$, where v_{turb} is the turbulent velocity in the point where terminal velocity is achieved (Lamers and Cassinelli (1999), p.20). For stars with strong winds main terminal velocity indicator lines are N V $\lambda\lambda 1239 - 43$, Si IV $\lambda\lambda 1394 - 1403$ and C IV $\lambda\lambda 1548 - 51$ doublet. In the FUV range strong indicator of terminal velocity is O VI $\lambda\lambda 1032 - 1038$ (Martins, 2010). These lines are fitted with synthetic spectrum and by obtaining the best fit we indirectly determine v_∞.

Mass-loss rate   There are various lines that can be used for mass-loss diagnostic. In UV range lines that can be used to derive mass-loss rate are strong UV lines such as C IV $\lambda\lambda 1548 - 51$, N V $\lambda 1240$, Si IV $\lambda\lambda 1394 - 1403$ (Bouret et al., 2012). UV lines are sensitive to product of wind density and ionization fraction of the respective ion. Density is related to mass-loss rate and from fitting those features we can determine mass-loss. UV lines used in mass-loss diagnostics have P-Cygni profile and their strength allows for determination of mass-loss as low as $10^{-10} M_\odot \ yr^{-1}$, which is important for the 'weak-wind stars' (Martins, 2010). However, UV lines have problem since if we want to constrain the value of mass-loss only by using UV lines we need to know ionization structure. This poses the main problem on mass-loss diagnostics from PV line. There are other lines in the FUV range that are available for this diagnostics, but they are often contaminated by interstellar atomic and molecular H absorption (Martins, 2010; Šurlan et al., 2013).

Clumping parameters   If only UV lines are present then from scattering lines in that range only the modified ionization structure clumping effect is present (the intensity linearly depends on density) (Martins, 2010). In this work, clumping parameters are obtained from P V $\lambda\lambda 1118 - 28$ resonance line. For detailed description of effect of clumping on different diagnostics, reader is referred to Fullerton (1997).

Chapter 3

Modeling of hot star atmosphere

3.1 Basic theory of stellar atmospheres

Atmosphere of the star is a very narrow, but yet important part of the star. All radiation observed from the star originates from stellar atmosphere. Atmosphere of the star is starting at the point with high temperature, density and where almost all atoms are ionized and its total mass is around $\approx 10^{-10} M_\odot$ (Mihalas, 1978). No matter how negligible its mass may seem, it is part of the star that gives us all information about the star itself. Without studying stellar atmospheres we would not know its chemical composition, whether or not the star has magnetic field, etc. This is due to the fact that all spectral lines used for spectral diagnostic are formed in the stellar atmosphere(Mihalas, 1978). However, from the spectrum itself we cannot say what is, for example, the exact temperature of the star and this is the reason why we need models of atmospheres. They give us synthetic spectrum, which we can then compare to observed one and find other parameters that are impossible to read from the observed spectrum.

Modeling of stellar atmosphere represents complicated problem and solving it requires much time and strong computers (and in bottom line money) and we need to simplify the situation. First simplification is to use certain symmetries to avoid dealing with 3 separate axis. There are two approximations used: plan-parallel and spherically symmetric approximation (Mihalas, 1978). Plan-parallel approximation is useful if size of the atmosphere is negligible compared to star's radius. In this approximation all physical parameters change just in one direction (usually marked as z). However, if star's atmosphere cannot be neglected, compared with its radius, spherically symmetrical approximation must be used. This approximation is used to describe dependence of physical quantities on distance r from the center of the symmetry. Key parameter in this approximation is cosine of the angle θ which is the angle between direction of propagation of radiation and radial direction: $\mu = \cos\theta$.

Every model of stellar atmospheres is solving the radiative transfer equation in order to produce as a final product synthetic spectrum which can then be compared to observed one. In order to derive the radiative transfer equation, the radiation field is assumed to be time-dependent. If material is assumed to be in rest then both
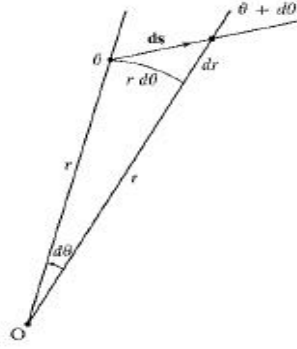
Figure 3.1: Geometry of spherically symmetric medium. Adopted from Mihalas (1978), Figure 2-2.

opacity[1] and emissivity[2] will be isotropic and vice-versa, in the moving material changes in photon's frequency and direction must be accounted for (which result from the transformation between the laboratory frame and the fluid frame). The difference between the amount of energy that emerges from volume element of length ds and cross-section dS and the incident one must be equal to the amount created by emission from the material in that volume element minus the amount absorbed.

$$[I(\mathbf{r} + \Delta\mathbf{r}, \mathbf{n}, \nu, t + \Delta t) - I(\mathbf{r}, \mathbf{n}, \nu, t)] \, dSdsd\omega d\nu dt =$$
$$[\eta(\mathbf{r}, \mathbf{n}, \nu, t) - \chi(\mathbf{r}, \mathbf{n}, \nu, t)] \, dSdsd\omega d\nu dt \qquad (3.1)$$

If we denote the path-length along the ray as s then $\Delta t = \Delta s/c$ and by simple algebra we obtain the **radiative transfer equation**:

$$\left[c^{-1}\frac{\partial}{\partial t} + \frac{\partial}{\partial s}\right] I(\mathbf{r}, \mathbf{n}, \nu, t) = \eta(\mathbf{r}, \mathbf{n}, \nu, t) - \chi(\mathbf{r}, \mathbf{n}, \nu, t)I(\mathbf{r}, \mathbf{n}, \nu, t) \qquad (3.2)$$

Spherical symmetry will be focus in further discussion, since the model used in this thesis (PoWR) is solving the radiative transfer equation in spherically symmetric approximation. In a spherically symmetric medium the specific intensity will be independent on coordinates that specify the direction of the beam relative to the local outward normal $\hat{\mathbf{r}}$. Therefore, instead of $I(\mathbf{r}, \mathbf{n}, \nu, t)$ we can write $I(\mathbf{r}, 0, \nu, t)$. However, we also have to know the general form of d$\mathbf{s}$ to be:

$$d\mathbf{s} = dr\hat{\mathbf{r}} + rd\theta\hat{\theta} \qquad (3.3)$$

As is seen from geometry $dr = \cos\theta ds$ and $rd\theta = -\sin\theta ds$ and the derivative $\partial/\partial s$ is now:

$$\frac{\partial}{\partial s} \to \cos\theta\frac{\partial}{\partial r}\sin\theta\frac{\partial}{\partial \theta} \qquad (3.4)$$

---

[1]describes the removal of energy by the material

[2]the amount of energy emitted by the material

If we say that $\cos\theta = \mu$ then we can rewrite the above equation as:

$$\frac{\partial}{\partial s} \to \mu\frac{\partial}{\partial r} + r^{-1}\left(1-\mu^2\right)\frac{\partial}{\partial\mu} \tag{3.5}$$

We can now write the radiative transfer equation for a spherically symmetric atmosphere:

$$\left[c^{-1}\frac{\partial}{\partial t} + \mu\frac{\partial}{\partial r} + r^{-1}\left(1-\mu^2\right)\frac{\partial}{\partial\mu}\right]I(\mathbf{r},\mathbf{n},\nu,t) =$$
$$\eta(\mathbf{r},\mathbf{n},\nu,t) - \chi(\mathbf{r},\mathbf{n},\nu,t)I(\mathbf{r},\mathbf{n},\nu,t) \tag{3.6}$$

The atmospheres of hot stars are expanding. The main consequence of this fact is that opacity and emissivity are becoming affected by the velocity field via Doppler shift. The static equation of radiative transfer can be used for calculation of continuum radiation in a moving frame since changes in opacity and emissivity coefficients are negligible in the region of the Doppler frequency shift. However, for lines this approach cannot be used. Equation of radiative transfer can be solved either in the observer's frame or in the co-moving frame.

Observer's frame (or often referred to as laboratory frame) is the frame of reference where the observer is at rest with respect to the center of the star. Advantage of using this frame is that the partial differential equations for radiation intensity are simple and any velocity field can be adopted and treated. However, in this frame opacity and emissivity are anisotropic (due to the velocity field) and angle and frequency are coupled. Great amount of frequency points are needed in order to correctly describe the line profile and due to this the velocity difference between two consecutive depth points has to be smaller several times than the thermal velocity. Generalized form of the radiative transfer equation in this frame looks like:

$$\left(\frac{1}{c}\frac{\partial}{\partial t} + \mathbf{r}\cdot\nabla\right)I(\mathbf{r},\mathbf{k},\nu_{obs},t) = \eta(\mathbf{r},\mathbf{k},\nu_{obs},t) -$$
$$\chi(\mathbf{r},\mathbf{k},\nu_{obs},t)I(\mathbf{r},\mathbf{k},\nu_{obs},t) \tag{3.7}$$

where $\mathbf{k}$ is the direction of propagation of radiation, ν_{obs} is the radiation frequency. The radiative transfer equations for static and moving media, in the observer's frame, are the same.

Co-moving frame, represents the frame that moves with the outflowing material. Opacity and emissivity, in this reference frame, are not affected by the velocity field and no additional anisotropy needs to be introduced. This fact, together with the fact that anisotropy on atomic level can be neglected is main reason why radiative transfer equation is solved in this frame. However, in order to compare lines calculated in this frame to the observed ones, calculated lines must be translated into the line of sight of the observer in infinity. Radiative transfer equation, neglecting relativistic effects and aberration in the co-moving reference frame and assuming that velocity is not too large can be written as:

$$\frac{1}{c}\frac{\mathrm{d}I}{\mathrm{d}t} + \mathbf{k}\cdot\nabla I(\mathbf{r},\mathbf{k},\nu_{cmf},t) - \frac{1}{c}\mathbf{k}\cdot\nabla\mathbf{v}\cdot\mathbf{k}\nu_{cmf}\frac{\mathrm{d}I(\mathbf{k},\nu_{cmf})}{\mathrm{d}\nu_{cmf}}$$
$$= \eta(\nu_{cmf},t) - \chi(\nu_{cmf},t)I(\mathbf{r},\mathbf{k},\nu_{cmf},t) \tag{3.8}$$

Another set of approximation deals with thermodynamics of atmosphere. We can talk about Local Thermodynamical Equilibrium (LTE) or non-LTE [3]. Main difference between two approximation is in the way how we calculate population numbers of certain energy levels. In LTE approach we use Saha's equation to describe ionization equilibrium:

$$\frac{N_j}{N_{j+1}} = n_e \frac{U_j(T)}{U_{j+1}(T)} \frac{1}{2} \left(\frac{h^2}{2\pi m_e kT} \right)^{3/2} \exp\left(\frac{\chi_{I,j}}{kT} \right) \tag{3.9}$$

where n_e is the concentration of free electrons, $U_j(T)$ and $U_{j+1}(T)$ are partition function of j and $j+1$ ionization level respectively, m_e is the mass of the electron, $\chi_{I,j}$ is the ionization potential and $\frac{N_j}{N_{j+1}}$ is tge ratio of concentration of two consecutive ions. Excitation equilibrium, in LTE approximation, is described by Boltzmann's equation:

$$\frac{n_{ij}}{N_j} = \frac{g_{ij}}{U_j(T)} \exp\left(-\frac{\chi_{ij}}{kT} \right) \tag{3.10}$$

where n_{ij} represents the population number of ith level of the ion j, g_{ij} is the statistical weight of given level and χ_{ij} is its ionization potential (Mihalas, 1978).

For hot stars, this approximation is not sufficient. In LTE approach it was assumed that the equilibrium is due to collision processes. In hot stars equilibrium is due mostly to radiation processes, but radiation field is not in equilibrium. Non-LTE approach has to be used in this case. Population numbers are then derived from the equations of statistical equilibrium which look like

$$\sum_{j \neq i} n_j P_{ji} - n_i \sum_{j \neq i} P_{ij} = 0 \tag{3.11}$$

where P_{ji} is the total transition rate from level j to level i. Total transition rate for transitions between levels i and j is: $P_{ij} = R_{ij} + Cij$, where R_{ij} represents radiation transitions and C_{ij} collision transitions. Even though, this equations look simple in form written above, we always must know that there are many atoms in atmospheres of stars, and each of those atoms can have many ions which can further have numerous levels. Dependence of R_{ij} of radiation is main complication of non-LTE approach. Solving the equation of statistical equilibrium requires numerical methods (Mihalas, 1978).

3.2   Challenges in modeling of stellar atmospheres

From the above written it is clear that modeling of hot star atmospheres is challenging task. First challenge is that atmospheres are dominated by a radiation field with energy densities larger or at least the same order as energy density of the atmospheric matter. This results in two consequences. First one is, already described, non-LTE approach and the second that supersonic hydrodynamic outflow of atmospheric matter is initiated by line absorption (Kudritzki and Puls, 2000). Line-blanketing effect is another reason why complex radiative transfer method is needed. The

---

[3]by this term is meant all departs from LTE

UV spectrum of hot stars is dominated by metallic lines. Due to this fact, the line-blanketing effects cannot be neglected and so-called "iron forest" has to be accounted for in codes. Today, there are various numerical models dealing with atmospheres of hot massive stars. Their comparison is given in the table 3.1.

Table 3.1: Characteristics of different stellar atmosphere codes

Characteristic	POWR	CMFGEN	FASTWIND
radiative transfer	comoving frame	comoving frame	CMF/Sobolev
line-blanketing	full	full	approximative
photosphere	quasi-hydrostatic	quasi-hydrostatic	quasi-hydrostatic
computation time	long	long	fast
geometry	spericall	spericall	sphericall

Modeling stellar atmosphere with unified models is complicated and time consuming. Unfortunately, many other problems are present in modeling stellar atmospheres. For O-type stars there are problems with β velocity exponent (from equation 2.2) Some stars are show to exhibit value of exponent β 0.5-1 times larger than predicted by radiation-driven theory (Hillier et al., 2003). Another problem that occurs is that calculation of radiation force requires knowledge of surface abundances which are determined in modeling. During modeling, need arose for another parameter in modeling O-type stars in order to match line strengths and line profiles from observation with synthetic model and to explain relative strengths of weak and strong metal lines belonging to the same elements. That parameter is called *microturbulent* velocity, but it is unclear what is the origin of it. In addition, there are evidences that in star exists the so-called *macroturbulent* velocity with values higher than local speed of sound. The names macroturbulence and microturbulence are adopted to help distinguish these two velocities, but also from our lack of knowledge what they essentially are. Real situation is that there is a continuum of scales, and full 3-D nature of the turbulent velocity field has to be taken into account in modeling line profiles. Information given in this paragraph, as well as more details, can be found in Hillier et al. (2003, 2012).

3.3 Potsdam Wolf-Rayet (PoWR) model atmosphere code

PoWR (Potsdam Wolf-Rayet) is a non-LTE model atmosphere developed at University of Potsdam. Code was firstly written for detailed analysis of WR stars, but in recent years the group of PhD students gathered around prof. Hamman is developing the code to be suited for analysis of O-stars as well. Primary assumption of the code is that the atmosphere is expanding in spherically symmetric, stationary flow. Mass-loss, density stratification and velocity field $(v(r))$ are connected via continuity equation (see equation 2.1). Velocity field used in code is pre-defined. In a subsonic part of the wind velocity is defined such that hydrostatic density stratification is

approached, while in supersonic part β-law is assumed, and terminal velocity v_∞ is considered as a free parameter. Inner boundary of the model is set to be "stellar radius" R_* which corresponds to Roseland optical depth of 20. Effective temperature T_{eff} is defined via Stefan-Boltzmann law. Code accounts for clumping in a so-called "microclumping" approach. In the profile function of line absorption coefficient only Doppler-broadening is accounted for (Hamann and Gräfener, 2004). The Doppler velocity v_D reflects random motion on small scales and it was firstly set ot 100 km s^{-1} for WR stars. For O-stars it is shown to be lower (see e.g. Sander et al. (2015)). Doppler velocity can be calculated as:

$$v_{dop} \approx \sqrt{\bar{v_{th}}^2 + v_{turb}^2} \tag{3.12}$$

In the above equation v_{th} represents the thermal velocity which is dependent on the specific atom and v_{turb} represents microturbulence. Thermal velocity $\bar{v}_{th} = \sqrt{\frac{2kT}{m}}$ is calculated for each element as depth-dependent in the formal integral, whereas co-moving calculations are currently done with constant v_{dop} for all elements. This fact does not influence much the synthetic spectra of WR stars, but for O-stars it has significant influence because it influence total radiative pressure in the atmosphere (Sander et al. (2015)). In the picture 3.2 is presented fitting of the optical lines sensitive to changes in Doppler velocity to different values of v_{dop}. In the figure 3.2 N lines represent lines sensitive to temperature. Bouret et al. (2012) reported on some inconsitencies in deriving T_{eff} from He lines with one derived from N lines, but that fitting of N lines cannot be achieved without degrading fit to the rest of optical and UV part of the spectrum.

In the modeling we fixed these values of Doppler velocity to $v_{dop} = 20$km s^{-1} and microturbulent velocity to $v_{turb} = 20$km s^{-1}.

Another important parameter for deriving the velocity field is the β - the velocity field exponent. Code used the so called double β law. The double-β-law (Hillier and Miller, 1999) is consisted of the sum of two β-law terms with different exponents β_1 and β_2, each of them contributing a pre-specified fraction to the total wind velocity. Compared to the standard "one-β" law, this one allows for a smaller velocity gradient in the lower part of the wind, while the second term, for which we adopt always $\beta_2 = 6$ and a contribution of 35% to the final velocity,causes some noticeable acceleration even at relatively large distances from the star (Šurlan et al., 2012). It is important to stress out that this form of velocity law is an approximation that fits the velocity distribution well, but it is not in any way the only possibility how to describe the velocity field. Example of velocity stratification in the model is given in figure 3.3.

PoWR is assuming spherically-expanding atmosphere. In this atmosphere equation of radiative transfer is formulated in co-moving frame, neglecting aberration and advection terms. The angle dependent equation of radiative transfer looks like:

$$\mu\frac{\partial I_\nu}{\partial r} + \frac{1-\mu^2}{r}\frac{\partial I_\nu}{\partial \mu} + \left[(1-\mu^2)\frac{v}{r} + \mu^2\frac{\mathrm{d}v}{\mathrm{d}r}\right]\frac{\partial I_\nu}{\partial x} =$$
$$\eta_\nu - \kappa_\nu I_\nu = \eta_\nu^{true} + \kappa_\nu^{Th} J_\nu - \left(\kappa_\nu^{true} + \kappa^{Th_\nu}\right) I_\nu \tag{3.13}$$

where x represents dimensionless frequency in Doppler units, while v and $\frac{\mathrm{d}v}{\mathrm{d}r}$ must be expressed in units of the corresponding reference velocity (Gräfener et al., 2002).
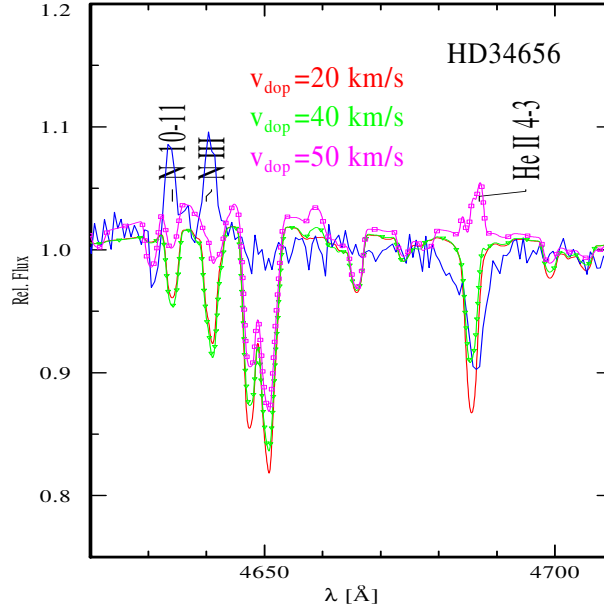
Figure 3.2: Fit of the optical part of the spectrum showing lines sensitive to changes in Doppler velocity for star HD 34656, obtained by PoWR. Blue thick line represents the observation.

Opacity and emissivity can split into a "true" and "Thomson" part. "True" terms on the right-hand side of the above equation can be calculated from non-LTE population numbers, the angle-averaged intensity J_ν in the scattering term includes intensities of different angles and it must be either taken from the preceding iteration , or the complete set of equations must be solved for all angles at the same time. Method used for solving this is the "method of variable Eddington factors", where Eddington factors used in the method are defined as:

$$f = \frac{K_\nu}{J_\nu} \text{ and } g = \frac{N_\nu}{H_\nu + \epsilon J_\nu} \tag{3.14}$$

Based on these factors, equation of radiative transfer is solved in each accelerated lambda iteration cycle by means of moment equations (Gräfener et al., 2002). In order to obtain convergence, it is necessary to accelerate the iteration by incorporating some approximate radiative transfer into the statistical equation. The overall convergence is stable, but not very fast and the computing time ranges from several hours to even couple of days on a modern workstation. PoWR produces synthetic spectrum by evaluating the formal integral (i.e., radiative transfer equation) in observer's frame (see equation 3.7).

For models with the same stellar effective temperature the strength of emission lines depends on a transformed radius which is defined as:

$$R_t = R_\odot \left[\frac{v_\infty}{2500 \text{km s}^{-1}} \middle/ \frac{\dot{M}\sqrt{D}}{10^{-4} M_\odot \ yr^{-1}} \right]^{\frac{2}{3}} \tag{3.15}$$
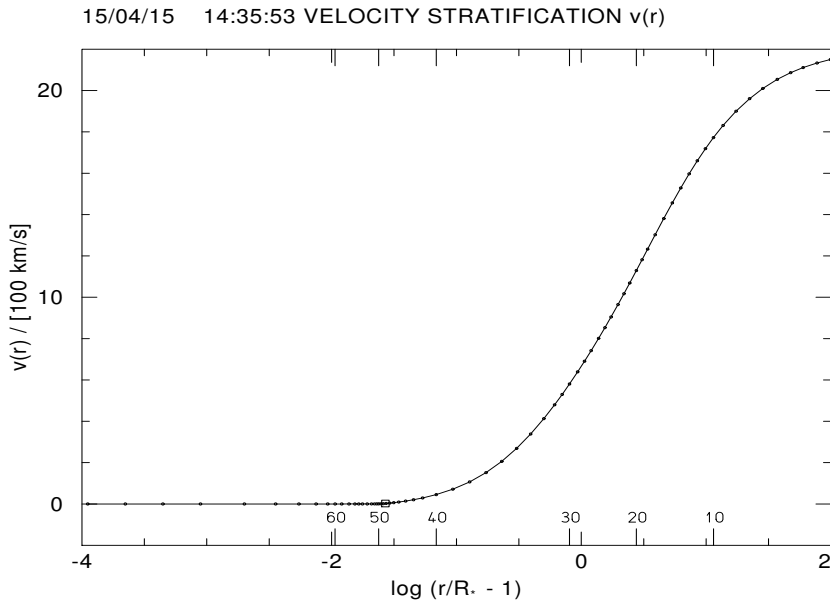
Figure 3.3: Velocity stratification

Figure 3.4: Example of velocity stratification in PoWR for one calculated model.

where $R_\odot$ represents the stellar radius (Gräfener et al., 2002; Hamann and Gräfener, 2004). Models are calculated using complex atomic data of H, C and N. Abundance of He is not predefined, it is calculated as difference between 1 (which represents the total sum of masses of all elements) and sum of element abundances predefined. Fe group elements are considered in the superlevel approach that accounts for $\sim 10^7$ line transitions between $\sim 10^5$ levels within 72 superlevels.

Scheme of the program flow is given in Appendix B.

3.4 3-D Monte Carlo Radiative Transfer code for inhomogeneous winds

Clumping is important factor in deriving correct mass-loss rate of stars that have strong clumped wind. Understanding of those processes is extremely important in astrophysics, in order to predict and estimate life cycle of stars. In order to incorporate clumping into already existing models of atmospheres it is crucial to deal with them in a 3-D way. As the theory evolved, from smooth wind models to clumped one series of approximations arose and one that stayed valid from the introduction of clumps is the one of treating clumping in the wind as 1-D or 2-D problem. First one to treat clumping as a 3-D problem and to incorporate it in solving of equation of radiative transfer were Šurlan et al. (2012, 2013). Model atmospheres developed earlier, for example above described PoWR, accounts for "microclumping" in a way that they define clumping factor D, which is free variable. This "microclumping" approach assumes that clumps are optically thin. There were various attempts how to solve discrepancies between mass-loss rate derived from H_α and PV line and the solution that was proposed is to use the "macroclumping" approach. By analogy, if "microclumping" assumes optically thin clumps, "macroclumping" is treating clumps as optically thick. Information about MCRT are taken from (Šurlan et al., 2012, 2013).

This code represents the 3-D code, that is using "macroclumping" approach and neglects approximation of void interstellar medium or monotonic velocity. In the developing of the code, wind model with possible smooth and clumped region was assumed. Parameter r_{cl} is introduced, which represents the distance where clumping in the wind sets on. The lowest boundary of the wind is set to the surface of star ($r_{min} = 1$). Region with values $1 \leq r \leq r_{cl}$ represents the smooth wind region, whereas the one with $r_{cl} \leq r \leq r_{max}$ represents the clumped wind region, where r_{max} represents the outer boundary of the wind. Model solves radiative transfer through the wind, and in doing so, it follows photons along their paths. The radiative transfer equation is solved in its dimensionless form. Dimensionless frequency in observers (x^{obs}) and co-moving frame (x^{cmf}) are introduced. During the calculations, the local co-moving frequency of the photon is kept, and this allows to express frequency of the followed photon at a certain coordinate point using the scalar product of the vector of local macroscopic velocity $\mathbf{v}$ and unit vector in the direction of the photon's propagation $\mathbf{k}$:

$$x^{cmf} = x^{obs} - \mathbf{k} \cdot \mathbf{v}. \tag{3.16}$$

When the photon exits the wind its frequency must be express as frequency in the observer's frame:

$$x^{obs} = x^{cmf} + \mathbf{k} \cdot \mathbf{v} \tag{3.17}$$

where $x^{obs} = \left(\frac{\nu}{\nu_0} - 1 \right) \frac{c}{v_s}$ where v_s represents an arbitrary reference velocity: $v_s = = \Delta \nu_s \frac{c}{\nu_0}$. Code is griddles and does not require any symmetry. Instead predefined grid, adaptive integration step Δr is introduced. After choosing this step, the velocity and opacity are calculated along the photon path. Vectors are described using the Cartesian coordinates. In order to study influence of clumping to resonance-line

Fixed model parameters	Varied model parameters
Outer boundary of the wind $r_{max}[R_\odot]$	Opacity parameter χ_0
Beta parameter β	Clump separation parameter L_0
Velocity at the photosphere v_{min} [km s^{-1}]	Clumping factor D
Terminal velocity v_∞ [km s^{-1}]	ICM density factor d
	Onset of clumping r_{cl}
	Doppler velocity v_D [km s^{-1}]
	Velocity deviation parameter $m = v_{dis}/v_\beta$

Table 3.2: Model parameters for studying influence of their variation on resonance line profiles.

formation core-halo model is adopted. Continuum opacity is neglected and only line opacity is taken into account in the wind. Only pure scattering (i.e., processes that does not involve absorption and re-emission of the photon) and Doppler broadening are considered and complete redistribution is assumed.

While other approaches and numerical codes assume clumps as either optically thin or thick, 3-D Monte Carlo radiative transfer for inhomogeneous winds allows for arbitrary depth of clumps, or in other words clumps can be optically think in the cores of resonance lines and optically thin in the rest of the wind. Assumption that is made is that the clumps are stochastically distributed in the wind. Two variables are used to describe clumps and their distribution. First one is the average clump separation $L(r)$ which is measured between centers of two clumps and depends with the distance r from the star. Other variable is radius of a particular clump l which also varies with the distance from the star $l = l(r)$, since for the simplicity clumps are assumed to have spherical shape. Density inside the clump (which also depends with the distance from the star) is assumed to be higher for a factor D (density contrast) than the smooth wind density at the same radius:

$$\rho_{cl}(r) = D\rho_{sw}(r). \tag{3.18}$$

Factor D has values $D \geq 1$ and is the free parameter, which for simplicity is assumed depth independent. It can be expressed using average clump separation $L(r)$ and clump radius $l(r)$ as:

$$D = \frac{L^3(r)}{\frac{4\pi}{3}l^3(r)}. \tag{3.19}$$

MCRT requires input set of parameters, such as mass-loss rate and ionization fraction. Those are derived for particular star with PoWR and serve as input parameters to MCRT from which are then derived parameters of clumps. Using this code it is possible to study how clumping affects singlet or doublet resonance lines. Depending on the effect that is studied some set of parameters is kept fixed, while other is varied. Table 3.2 gives set of fixed parameters (on the left side) and varied parameters (on the right side) for a typical O-type star.

Chapter 4

Studied stars and their observations

In this thesis we analyzed two Galactic O-type stars, HD 34656 with strong and HD 188001 with thin wind. Stars with strong wind have high mass-loss rate and H_α line profile exhibits emission peak. These stars are assumed to have highly clumped wind. Contrary to this, stars with thin wind have low mass-loss rates, emission from such winds is very small. Absorption lines are dominant and wind clumping is not pronounced (for more details see Puls et al. (1996)).

Since the main goal of the thesis is to determine wind and clumping parameters and to compare determined parameters for stars with strong and thin winds, selected stars are good examples.

4.1 HD 34656

HD 34656 is an O7II(f) star located in the Auriga OB2 association (Maiz-Apellaniz et al., 2004). This star was observed photographically by Slettebak (1969), while Garmany et al. (1980) concluded that it is a single star.

Fullerton et al. (1991) found small radial velocity variations in this star and inferred that it could be due to radial pulsation. Herrero et al. (1992) derived stellar parameters ($T_{\mathrm{eff}} = 39$ kK , $\log g =3.5$, e$=0.2$ and $v \sin i =85$ km s^{-1}) for this star using plan-parallel NLTE model atmosphere with H and He in hydrostatic and radiative equilibrium with no line-blanketing. In the same paper Herrero et al. (1992) are inferring that "...there is no reason to think that the high He abundance is in error by more than our standard errors".

Recently, Markova et al. (2004) analyzed the star to check to what extent the analysis of H_α profiles alone can provide results consistent with those originating from a complete spectral analysis. Investigation was done by approximate method derived by Puls et al. (1996) which was modified in order to account for line blanketing. It was found that derived value for M_v and R was inconsistent with its spectral type and in further analysis the star was denoted as "peculiar object". Values of parameters derived in this paper are: $T_{\mathrm{eff}} = 34.7$ kK, $\log g = 3.50$, $\log \dot{M} = $ -6.21 $M_\odot$ yr^{-1} and $v_\infty = 2150$ km s^{-1}.

Two years later Puls et al. (2006) re-examined this star and also marked it as "peculiar". Puls et al. (2006) found that this object has radio mass-loss rate larger

than the one derived from H_α and suggested possible explanations as:

a) it is a non-thermal emitter,

b) their measurements are somehow corrupted or

c) the outer wind is heavily clumped then inner one.

Analysis was done by combining H_α, IR, mm and radio fluxes, and using approximate methods, calibrated to more sophisticated models. Clumping was included in "conventional" way, assuming the inter-clump matter to be void. Most important result of that particular study is that for denser winds, the innermost region is strongly clumped than outer wind. Parameters derived in mentioned paper are T_{eff} = 34.7 kK, $\log g$ = 3.50, $\log \dot{M}$ = -5.58 $M_\odot \ yr^{-1}$, v_∞ = 2150 $\mathrm{km\,s^{-1}}$ and β = 1.09.

Most recent study of this star is done by Martins et al. (2015) who derived new set of values for C,N,O abundances. Using CMFGEN model atmosphere code, optical spectra were analyzed and determined stellar parameters of the star are T_{eff} = 36 kK and $\log g$ = 3.75.

4.2   HD 188001

HD 188001 or 9 Sge is O7.5Iab star (Sota et al., 2011). It is located in the constellation of *Saggita* (not to be confused with more famous one- Sagittarius).

Aslanov et al. (1984) searched for relativistic companions of OB runaways. Same authors detected spectrum variability and possible periodicity in radial velocity was detected for each of the stars from the sample in which one of the star was HD 188001. From those measurements authors concluded that it was a possible binary system with period of 78.3 days. Aslanov and Barannikov (1992) proposed that HD 188001 was an eclipsing binary system, with low-mass companion ($\approx 1.5\mathrm{M_\odot}$). In the same paper authors used spectroscopic and photometric WBVR observation which confirmed a period variability of the radial velocities and luminosity.

Underhill and Matthews (1995) re-examined question of the binarity of this star. Stars in the studied sample by these authors were observed at 30 $\mathrm{\mathring{A}}mm^{-1}$ in the blue-violet, yellow-green and red regions. Period for this star was estimated by Fourier analysis of all of the radial velocities obtained. Underhill and Matthews (1995) inferred that HD 188001 was a binary system with a possible companion of A-type or later, which was too faint to be observed in spectra of HD 188001. Mass of the companion they derived was in accordance with previously derived by Aslanov and Barannikov (1992).

Even now it is not clear enough if this star is a binary or not. For example in the database Simbad it is said that it is an eclipsing binary system, however, McSwain et al. (2007) examined the radial velocity of the star and from analysis compared with previous measurements they derived the conclusion: "...that HD 188001 is actually a single star, possibly with variable winds that contaminate He absorption lines and mimic the signature of a spectroscopic binary". In the analysis of radial velocities McSwain et al. (2007) used mainly He I and He II lines from 105 radial velocities measurements, but also acknowledged that these lines are affected by stellar wind.

HD 188001 was included in the study of Martins et al. (2015). Parameters derived in the study for this star are T_{eff} = 33 kK, $\log g$ = 3.35 and from personal

communication with the second author of the paper, Herve, A., wind parameters used in the study were obtained.

4.3 Observations

We are examining stars in 2 ranges: UV and optical. For UV range we used FUSE and IUE data, while both stars were observed with 2-m Ondřejov telescope.

Optical data   Both stars were observed in H_α region and blue part of spectrum. Those regions were observed with CCD SITe ST-005 800x200 px camera which is attached to Coudé spectrograph at 2-m Ondřejov telescope with slid width of 0.6". Angle of grating were set to 30:15 (centered at H_α line) with spectral resolution of 13 600 and 38:13 (covering HeII λ4686 and H_β lines) with spectral resolution of 19 400. For star HD 34656 observing conditions were better and spectral region around H_γ is recorded, while for star HD 188001 due to worsening weather condition only spectral lines around H_α and H_β were recorded. Telluric features in the spectra were removed using spectra of fast rotating star 116Tau (for star HD 188001 telluric correction was optimized for region around H_α, telluric lines around λ6300 Å are not well removed). Both spectra were wavelength calibrated with ThAr comparison. Data reduction was performed using IRAF by colleague from Estonia Anna Aret. Observational logs are given in table 4.1.

Table 4.1: Optical observation logs.

Star	Optical			
HD	UT date	UT start	$t_{\exp}[s]$	wavelength [Å]
34656	2012-12-29	18:38:21	2700	6254-6764
		19:29:50	3600	4754-5005
		20:37:24	3600	4270-4522
		21:47:16	3600	4557-4809
188001	2014-03-29	03:12:20	2100	4656-4907 H_β
		03:52:48	600	6254-6764 H_α

UV data   UV spectra were recorded by two satellites: IUE and FUSE.

IUE satellite was able to observe stars in wavelength range 1150-3200 Å both at high $(0.1 - 0.3\text{Å})$ and low $(6 - 7\text{Å})$ resolution. IUE satellite was functional from January 1978 until September 1996. In its almost 20 year career it obtained over 104 000 UV spectra. Spectra obtained with this rocket are available for free download either at https://archive.stsci.edu/iue/ or http://sdc.cab.inta-csic.es/cgi-ines/IUEdbsMY. For both stars we used short wavelength (SWP - Short Wavelength Prime Camera) and long wavelength (LWR - Long Wavelength Redundant Camera) high-resolution eschelle spectra.

FUSE was originally project of NASA. It was launched 3 years after IUE finished its mission. It operated from 1999 until the year 2007. Its primary role was to

use high-resolution spectroscopy in the FUV spectral region in order to explore the Universe. Comparing to the IUE it obtained small number of spectra (6000 of them), but it also worked 10 years shorter. Spectra of nearly 3000 objects are now publicly available at: https://archive.stsci.edu/fuse/search.php. FUSE covered the spectral region of PV resonance doublet line and therefore spectra obtained by it are important for this thesis.

All of the observed spectra were normalized using model continuum calculated from PoWR. Observation logs for UV data are given in table 4.2.

Table 4.2: FUSE, and IUE observation logs.

Star	FUV		NUV	
HD	Data set	UT date	Date ID	UT data
34656	P1011301000	2000-03-01	SWP40816HL	1991-02-04
			LWR12004RL	1981-11-20
188001	E0820901000	2004-05-29	SWP38942RL	1990-05-31
			LWR01682LL	1978-06-17

Chapter 5

Results of spectroscopic analysis

After we prepared optical, FUV and NUV data of both stars we performed the following procedure:

a) stellar and wind parameters were adopted from literature; b) 1-D models were calculated with the PoWR code assuming clumped wind. If achieved fit was not satisfactory, adopted parameters were varied in order to find the best fit between observations and synthetic spectra; c) the mass-loss rates were established from fitting the H_α line; d) then, the obtained mass-loss rate, the P V ionization fraction, and the photospheric spectrum were used as input for the 3-D Monte Carlo simulations of the clumped wind in order to determine the clumping parameters by optimizing the fit of the P V resonance doublet.

The synthetic spectra of both stars were flux-convolved to simulate instrumental and rotational broadening, taking $v \sin i = 85$ km s^{-1} for HD 34656 (see Markova et al. (2004)) and $v \sin i = 94$ km s^{-1} for HD 188001 (see McSwain et al. (2007)). Detailed model atoms of the most relevant elements (H, He, C, N, O, Si, P, Fe, and Fe-group elements) are taken into account in model calculations (see Gräfener et al. (2002)). The superlevel approach of Gräfener et al. (2002) was used to treat Fe-group line blanketing. We adopted mass fractions of H for HD 34656 from Puls et al. (2006) and for HD 188001 we were unable to find corresponding value of H abundance in literature and H abundance of the star of same type and spectral class (HD 192639) was adopted from Bouret et al. (2012). We recalculated their abundances of He given by number relative to hydrogen to mass fractions, and the abundance of H is then calculated as the rest, see Table 5.4. For the mass fractions of Si, P, and Fe-group elements we adopt the solar values determined by Asplund et al. (2005), see Table 5.4.

As input to the 1-D PoWR model calculations, we used the stellar and wind parameters and element abundances shown in Table 5.3, 5.5.

Table 5.1: UBVJHK photometry taken from the GOS catalogue (Maiz-Apellaniz et al., 2004)

Star (HD)	Other name	Spectral type	U	B	V	J	H	K
34656	...	O7II(f)	5.87	6.77	6.76	6.637	6.634	6.676
188001	9Sge	O7.5Iab	5.313	6.240	6.225	6.111	6.147	6.171

Table 5.2: Distances, reddening, extinction and absolute magnitude

Star (HD)	Distance (kpc)	Reddening	Extinction	Abs. magnitude	Source
34656	3.20	3.40	0.31	-6.79	1
188001	2.58	3.18	0.32	-7.52	2

References: Distance, reddening, extinction and absolute magnitude taken from 1 – Puls et al. (2006); 2 – McSwain et al. (2007).

Table 5.3: Input stellar parameters

Star (HD)	T_{eff} (kK)	R_* ($R_\odot$)	$\log L$ ($L_\odot$)	$\log g$	Source
34656	34.7	25.5	3.50	5.93	1
188001	33.0	20.186	3.35	5.94	2

References: Stellar parameters taken from 1 – Puls et al. (2006); 2 – Martins et al. (2015).

Table 5.4: Element abundances by mass-fraction for HD 34656

Element abundances (mass fraction)	H	C	N	O	Si	P	Fe	Sources
HD 34656	0.68	2.365 E-3	6.929 E-4	5.733 E-3	6.650 E-4	5.825 E-6	1.206 E-3	1,2
HD 188001	0.571	2.365 E-3	6.929 E-4	5.733 E-3	6.650 E-4	5.825 E-6	1.206 E-3	3,2

References: Value of H abundance taken from 1 – Puls et al. (2006) and 3 – Bouret et al. (2012); abundance of C, N, O, Si, P and Fe taken from 2 – Asplund et al. (2005).

Table 5.5: Input wind parameters

Star (HD)	$\log \dot{M}$ ($M_\odot\ yr^{-1}$)	v_∞ (km s^{-1})	β	Source
34656	-5.58	2150	1.09	1
188001	-5.9	1800	2.0	2

References: Wind parameters taken from 1 – Puls et al. (2006); 2 – Herve,A. (personal communication).
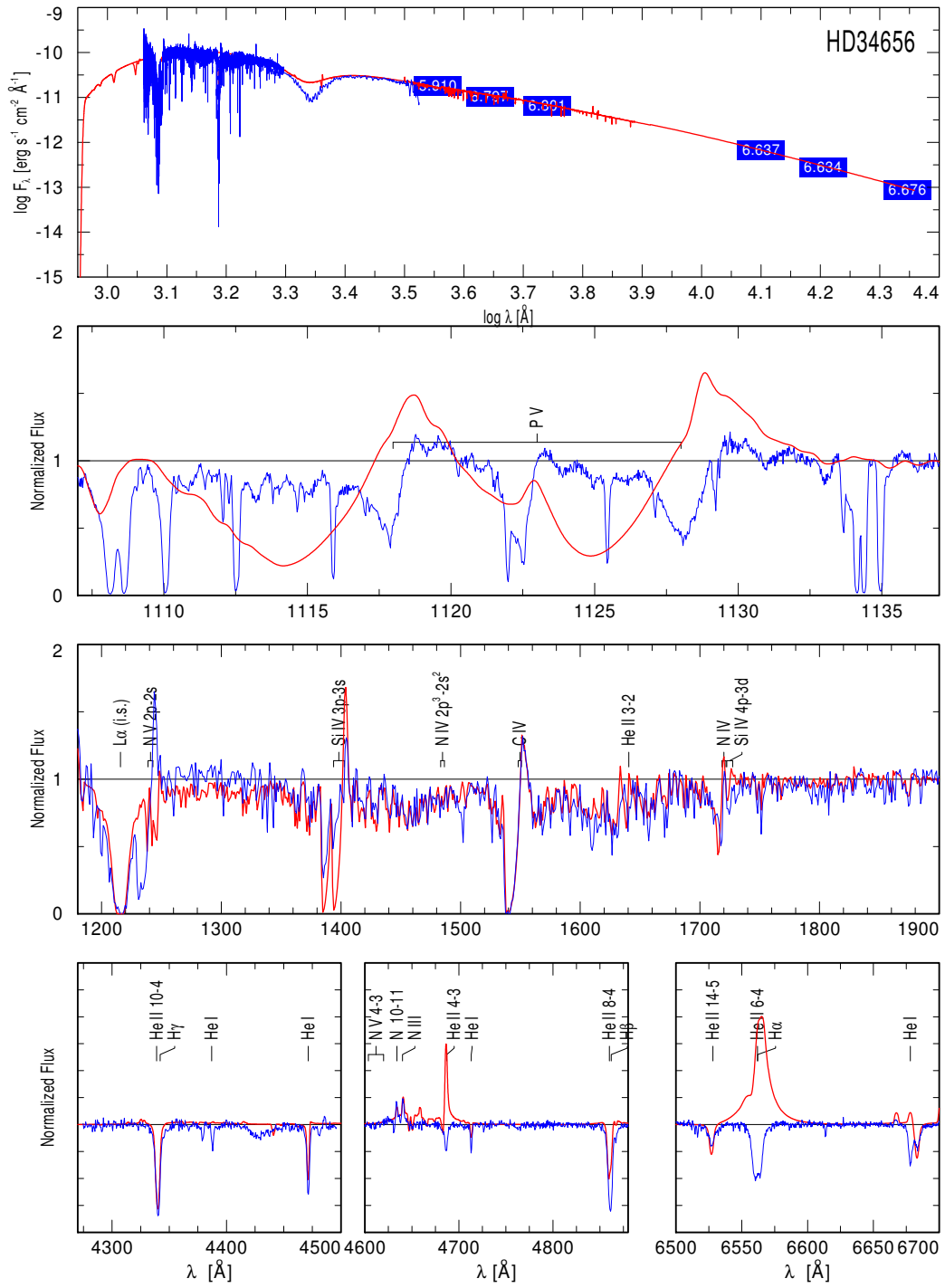
Figure 5.1: Fit from PoWR modeling (thick red solid line) to the observed HD 34656 spectra for stellar and wind parameters found in Puls et al. (2008). Blue labels with numbers in the uppermost panel are UVBJHK magnitudes.
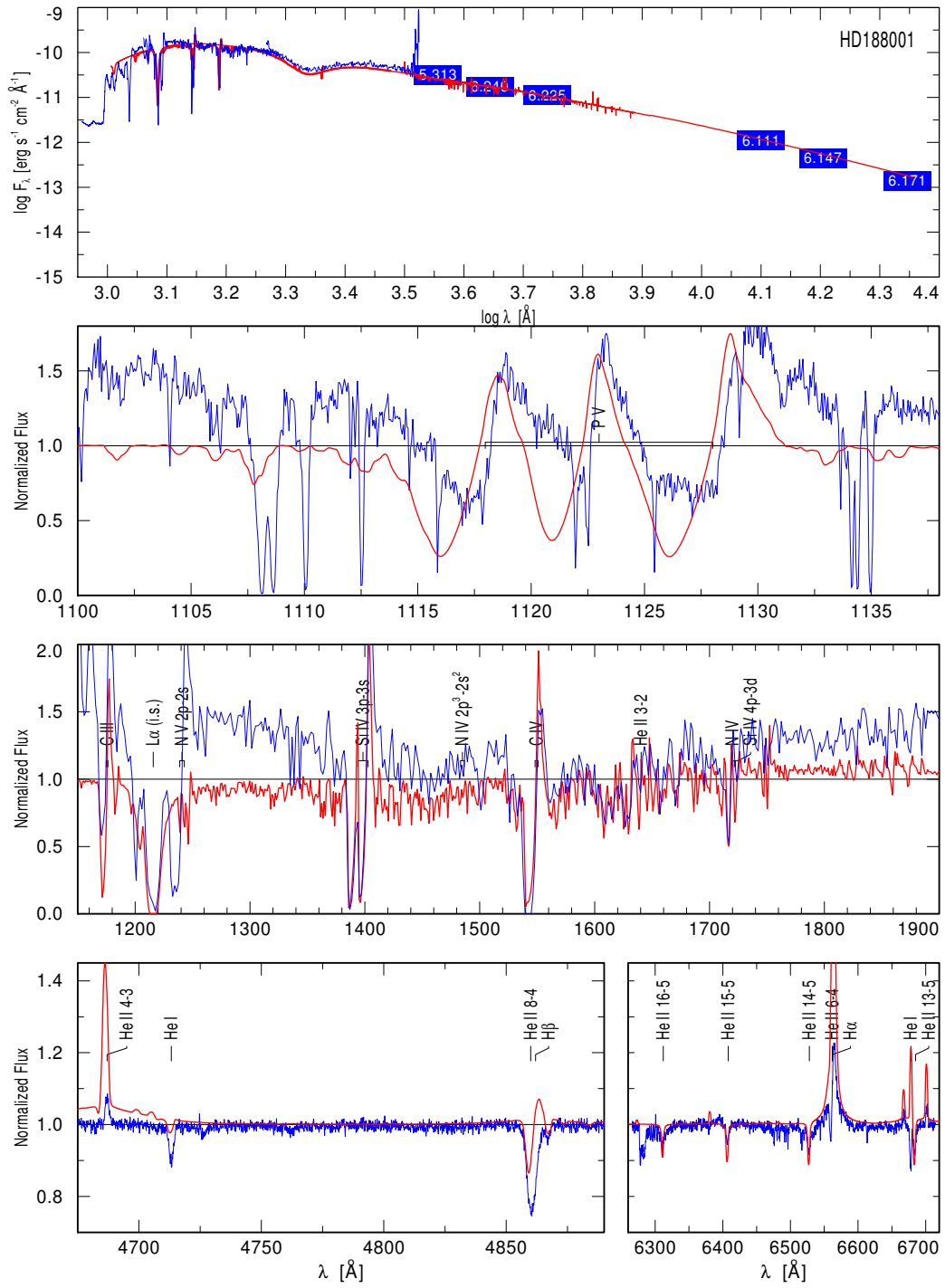
Figure 5.2: Fit from PoWR modeling (thick red solid line) to the observed HD 188001 spectra for stellar and wind parameters found in Martins et al. (2015). Blue labels with numbers in the uppermost panel are UVBJHK magnitudes.

5.1 Stellar parameters

5.1.1 Stellar luminosity

Spectral energy distribution (SED) fitting is becoming the standard way of deriving the stellar luminosity. It uses spectrophotometry from the (far)UV to infrared in order to adjust the global flux of atmosphere models. This method also has an advantage that the reddening (R_V) can be derived simultaneously. However the distance from the star must be known independently. In the pictures below examples of SED tting for both stars in the stellar sample are shown. Galactic reddening law used is described in Cardelli et al. (1989).

The UBVJHK photometry of stars is listed in Table 5.1, distances, interstellar extinction and reddening are listed in Table 5.2. We applied the reddening law from Cardelli et al. (1989) and adjusted the RV parameter to optimize the fit between the spectral energy distributions (SED) of the models and the flux-calibrated observations. The luminosities and distances of the stars we kept at the literature value, and we adjusted reddening and interstellar extinction to achieve the SED fits. Our final values for RV and the stellar distance are listed in Table 5.8. The SED fits are documented in the most upper panels of figures 5.1 and 5.2 .

After the first model was calculated we obtained unsatisfactory fit. In Fig. 5.1 it can be seen that synthetic spectrum deviates much from observations. Especially the H_α line since it is observed in absorption and the synthetic spectra shows the line in emission. The synthetic P V line appears in stronger absorptions. The main reason and explanation of such deviation could be clumping. Since the stellar and wind parameters taken from Puls et al. (2006) were determined assuming smooth wind, given mass-loss rate was overestimated. Therefore we adjusted the mass-loss rates to optimize the fit with the optical observations (H_α, H_β, H_γ, and He II lines). Models with different values of mass-loss rates were calculated assuming microclumping with clumping factor D=10. Final spectral fit is shown in Fig. 5.3.
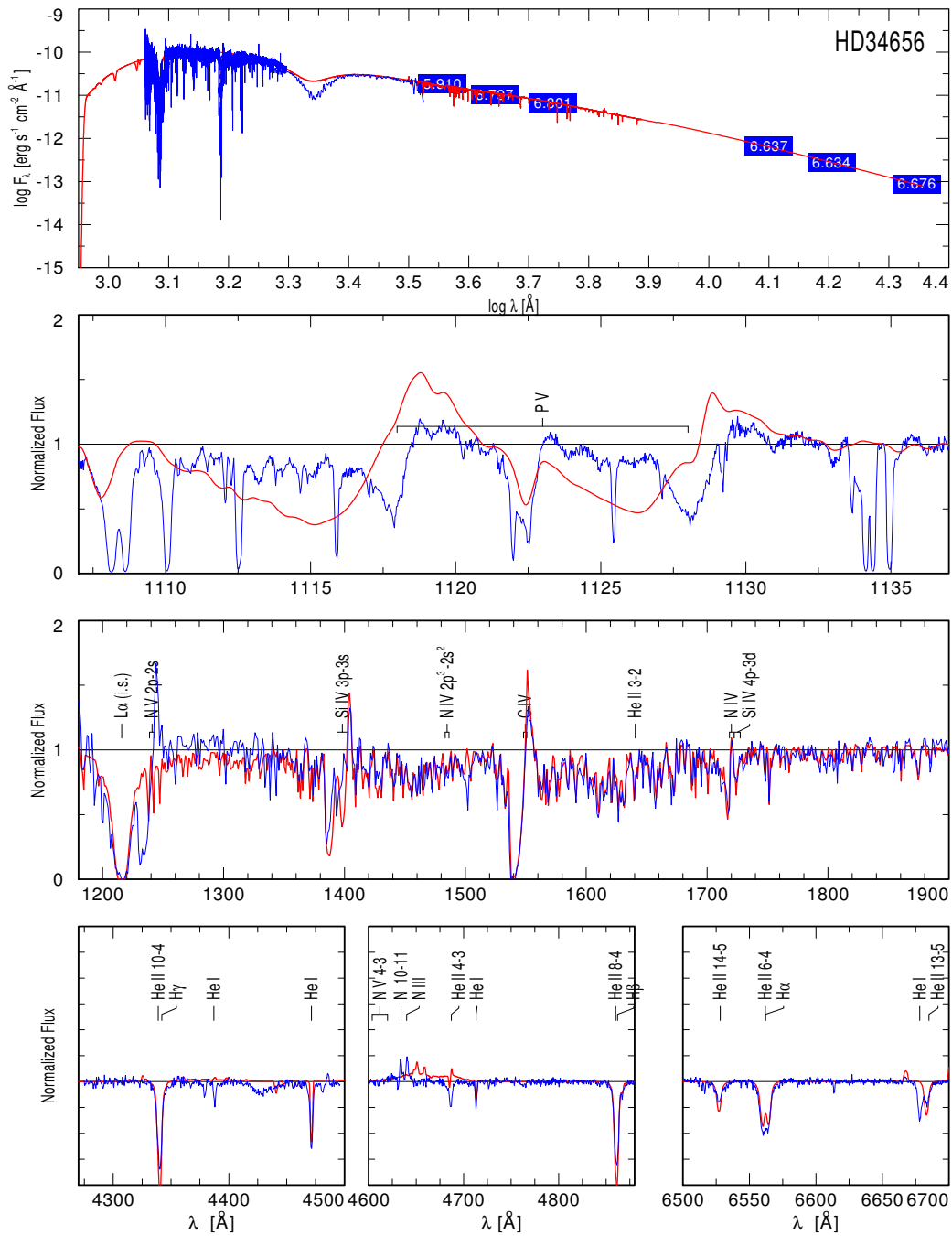
Figure 5.3: Fit from PoWR modeling (thick red solid line) to the observed HD 34656 spectra for value of mass-loss rate $\log \dot{M} = -6.2$. Thick blue line represents observation, while red one represents PoWR model.

Spectral fit with literature values of stellar and wind parameters for HD 188001 is shown in Fig. 5.2. Again it is seen that synthetic spectrum deviates from ob-

servations, especially FUV and NUV (panels 2 and 3, respectively) and that the SED is not fitted satisfyingly. Reason for this, is the temperature. Since in order to reproduce satisfactory fit for SED we need luminosity, reddening and distance. For the values of reddening and distances derived, luminosity obtained by Martins et al. (2015) is overestimated. Since the luminosity scales with T_{eff}^4 and, as is seen on bottom panels of Fig. 5.2, synthetic spectrum of He lines used for temperature diagnostics (see Section 2.4.1 and 5.1.2) is stronger than observed one we deduced that the T_{eff} is overestimated and its value needs to be lowered.

5.1.2   Effective temperature

In Fig. 5.1 and 5.2 can be seen that He I $\lambda6678$ and He II $\lambda6408$ lines in red part of the spectra and He I $\lambda4471$ and He I$\lambda4713$ lines in blue part of the spectra which represents the good temperature diagnostic are not fitted very well. Therefore, we decided to vary T_{eff} in order to obtain satisfactory fit with these lines. In Fig. 5.4a and 5.4b are shown line profiles of the He I (navesti lambda) and He I (navesti lambda) lines calculated with different values of T_{eff} for HD 34656. The lowest value of temperature gives the strongest lines in the synthetic spectra. As the value of temperature is increased the strength of the He I lines is weakened. If we then continue to increase the value of the effective temperature then we will, in these two examples, obtain He I lines in emission rather than in absorption as is observed. For further modelling value of T_{eff} =33 kK was used since it gives the most satisfactory fit with T_{eff} diagnostic lines.
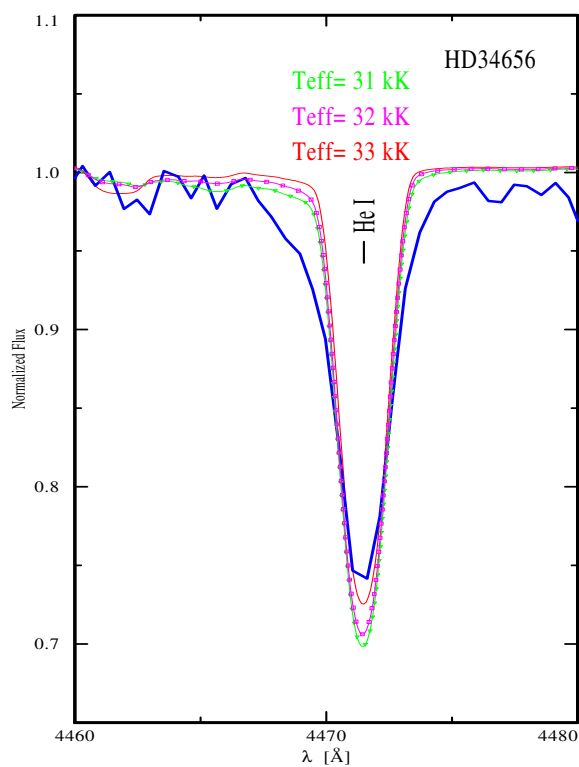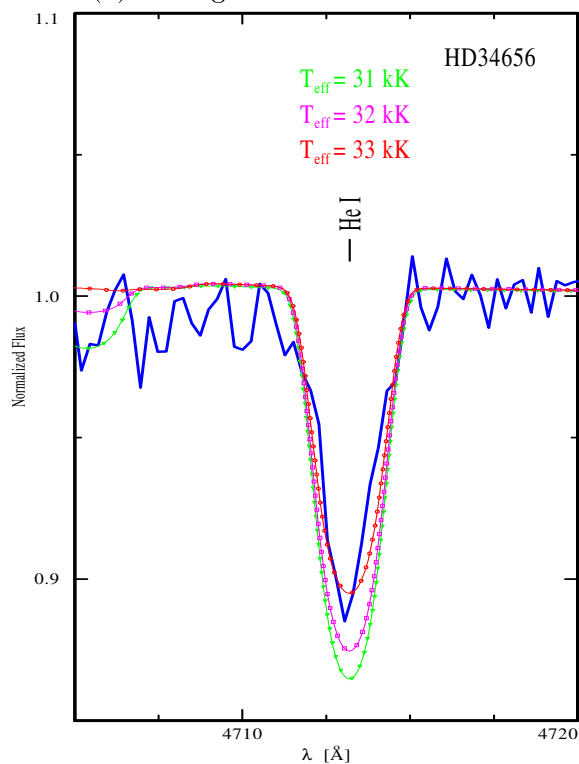
(a) Fitting of the HeI λ4471 line

(b) Fitting of the HeI λ4713 line

Figure 5.4: Line profiles of the He Iλ4471 and the He I λ4713 line calculated with different value of $T_{\rm eff}$ for star HD 34656. Blue full line represents the observation, while other lines represent line profiles calculated with PoWR for $T_{\rm eff}$ =31 kK (green line with triangle), $T_{\rm eff}$ =32 kK (violet line with squares), and $T_{\rm eff}$ =33 kK (red line with circles).

Unfortunately, for star HD 188001 part of the optical spectrum containing line He I λ4471 was not observed and due to that we used only He I λ4713 for estimating the value of effective temperature. Line profile of He I λ4713 and calculated line profiles for different values of T_{eff} are shown in Fig. 5.5. Changing of the values of T_{eff} produces the same effect as for the star HD 34656. For further modeling, value of $T_{\text{eff}} = 32.5$ kK was used, since it gives the most satisfactory fit with T_{eff} diagnostic line.
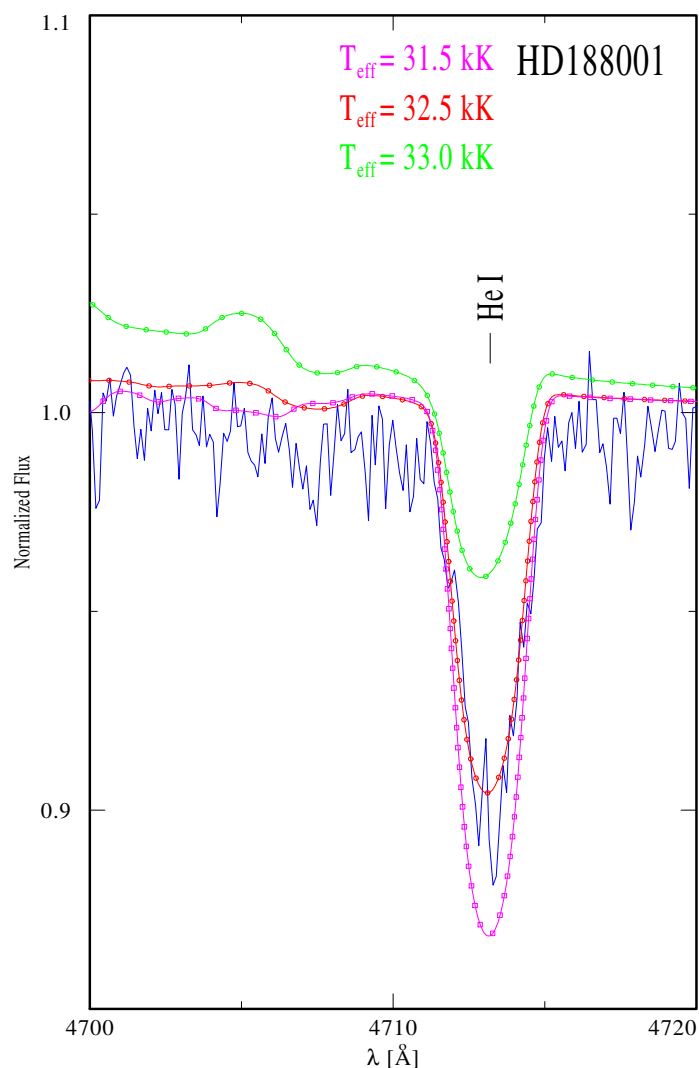
Figure 5.5: Line profiles of the He I λ4713 lines calculated with different value of T_{eff} for star HD 188001. Blue full line represents the observation, while other lines represents line profiles calculated with PoWR for T_{eff} =31.5 kK (violet line with squares), T_{eff} =32.5 kK (red line with circles), and T_{eff} =33 kK (green line with triangle).

Values of T_{eff} derived using PoWR code are about 1000 K lower than the values found in literature for both stars and are listed in Table 5.8.

5.1.3   Surface gravity

For surface gravity determination the main diagnostics are Balmer lines (see section 2.4.1). To check if adopted values of surface gravity from literature are correct for both analyzed stars $\log g$ was varied to see how different values of $\log g$ affect H_γ and H_β line profiles. Result for HD 34656 is shown in Fig. 5.6a and 5.6b. When value of surface gravity is increased depth and width of the H_γ and H_β lines increase. For the value of $\log g = 3.0$ the lines are more narrow and less deep than for other two values. The values of $\log g = 3.5$ and $\log g = 3.7$ are giving similar fit. Similar results in varying log g we also obtained for HD 188001.

Since we did not found uncertainties in $\log g$ determination we have decided to keep value $\log g = 3.5$ for HD 34656 and $\log g = 3.35$ for HD 188001 found in literature.
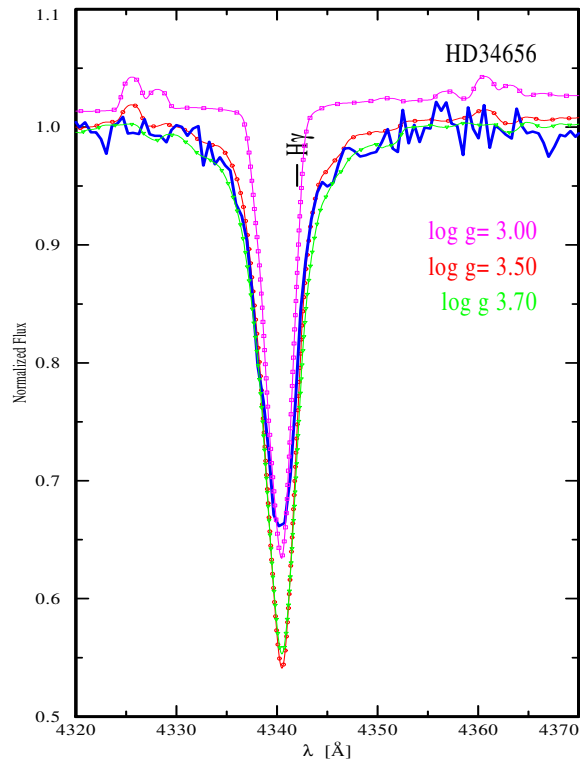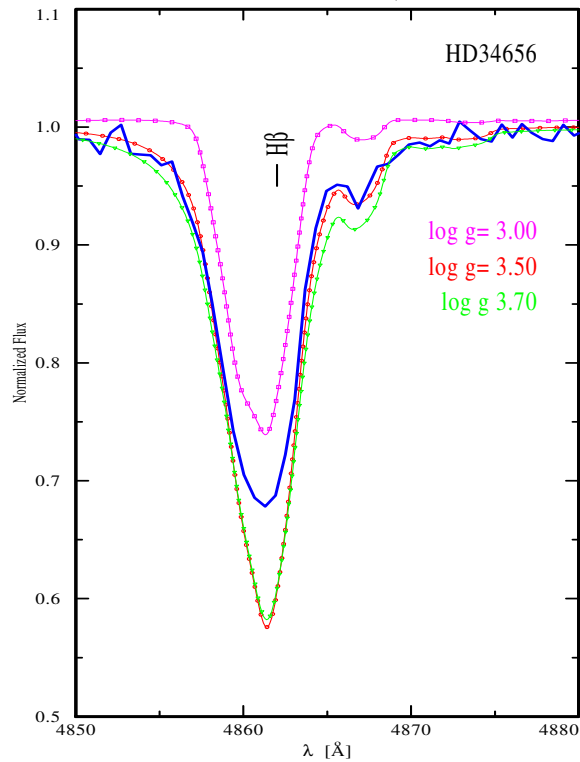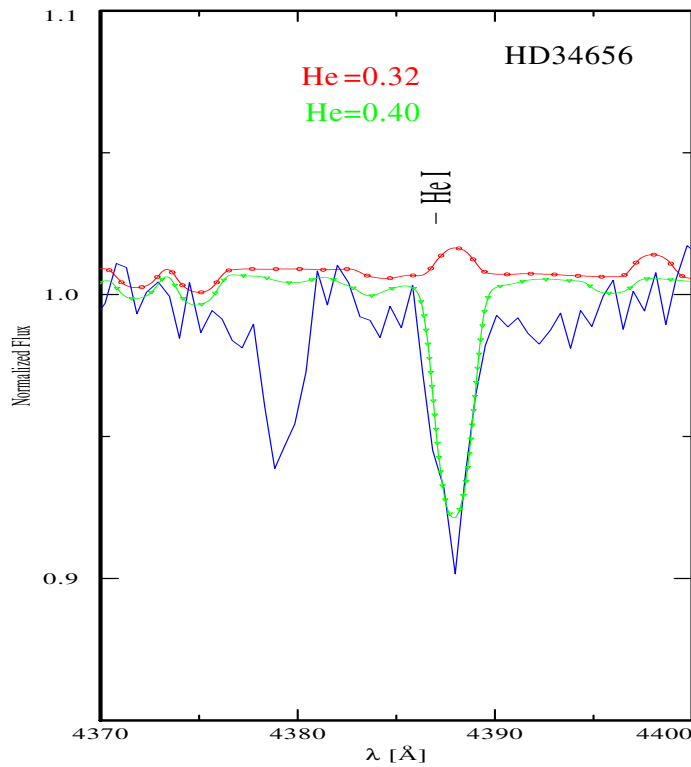
(a) Fitting of the H_γ line
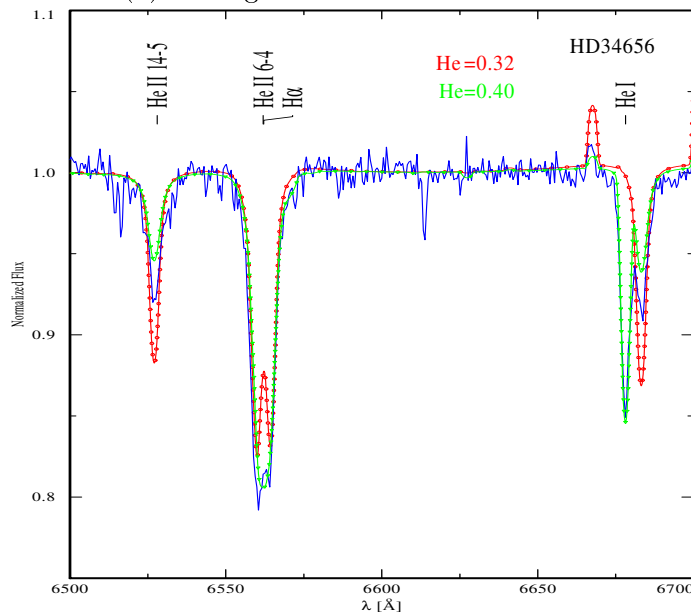

(b) Fitting of the H_β line

Figure 5.6: Line profiles of H_β and H_γ lines calculated with different value of $\log g$ for the star HD 34656. Blue full line represents the observation, while other lines represents line profiles calculated with PoWR for $\log g$=3.00 (violet line with squares), $\log g$=3.50 (red line with circles), and $\log g$ =3.70 (green line with triangle).

5.1.4   Surface abundaces

In order to improve the fitting of He lines, especially He I λ4387, He I λ6678 and He II λ4687, He II λ6528 lines, we tried to change value of He abundances of both stars . In Fig. 5.7a and 5.7b are shown line profiles with different values of He abundances.

(a) Fitting of the He I λ4387 line with different values of He abundance.

(b) Fitting of the He II λ6528 and He I λ6678 lines with different values of He abundance.

Figure 5.7: Line profiles of the blue and the red part of the optical spectra calculated with different value of He abudance for the star HD 34656.Blue full line represents the observation, while other lines represents line profiles calculated with PoWR for He mass fraction of 0.32 (red line with circles) and 0.40 (green line with triangle).
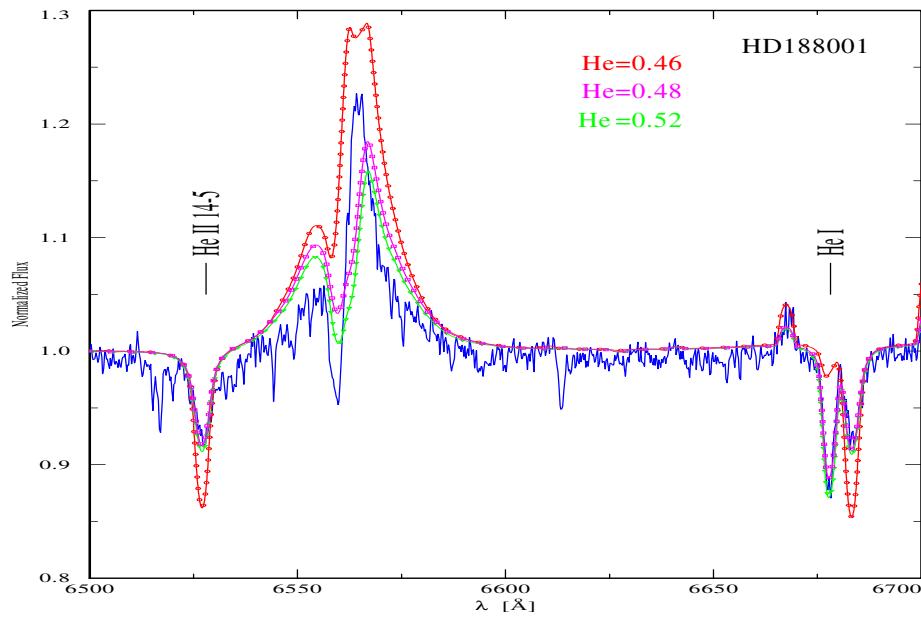
Figure 5.8: Line profiles of the blue and the red part of the optical spectra calculated with different value of He abudance for the star HD 188001.Blue full line represents the observation, while other lines represents line profiles calculated with PoWR for He mass fraction of 0.46 (red line with circles), 0.48 (violet line with squares) and 0.52 (green line with triangle)

From Fig. 5.7a, 5.7b and 5.8 is seen that changing the abundance of He improves fit of several lines, especially He I λ6678. However, since the primary focus of this thesis is not deriving surface abundances, values found in literature for H and He abundance are kept in all further modeling.

5.2   Wind parameters

5.2.1   Terminal velocity

As it is explained in subsection 2.4.2 for determination of terminal velocity it is good to use UV saturated lines like C IV resonance line. In this thesis value for v_∞ adopted from literature (listed in Table 5.5) was used. To show how changes of v_∞ influence synthetic spectra three models for different values of v_∞ were calculated.

Results are shown in Fig. 5.9 for the star HD 34656. If the value of v_∞ is low, the spectral line becomes more narrow and absorption part of the P Cygni profile cannot be fitted. On the other hand, if the value of v_∞ is high, the line becomes wider and absorption part of the P Cygni profile cannot be fitted. Similar results were obtained also for HD 188001. From checks we preformed, we decided to keep adopted values of v_∞ of both stars from literature.
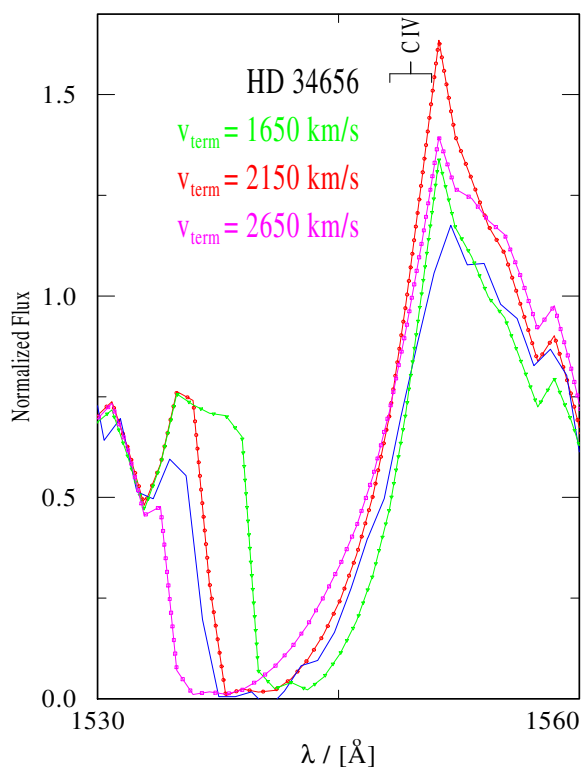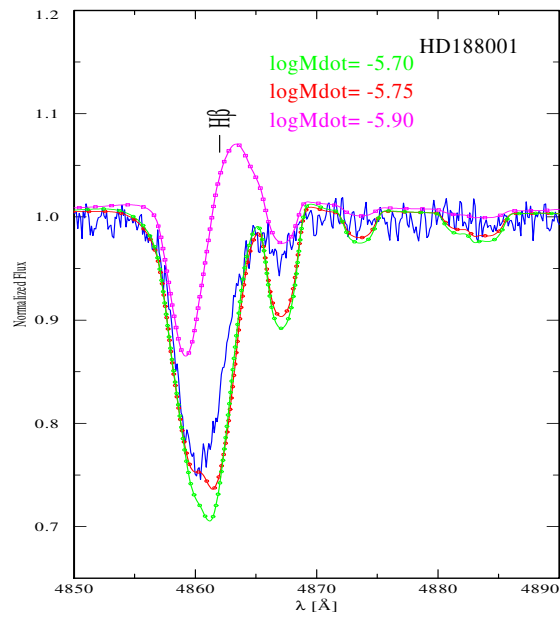

Figure 5.9: Line profiles of the C IV line calculated with different value of He abudance for the star HD 34656.Blue full line represents the observation, while other lines represents line profiles calculated with PoWR for value od v_∞ of 1650 $\mathrm{km\,s^{-1}}$ (green line with triangle), 2150 $\mathrm{km\,s^{-1}}$ (red line with circles) and 2650 $\mathrm{km\,s^{-1}}$ (violet line with squares).
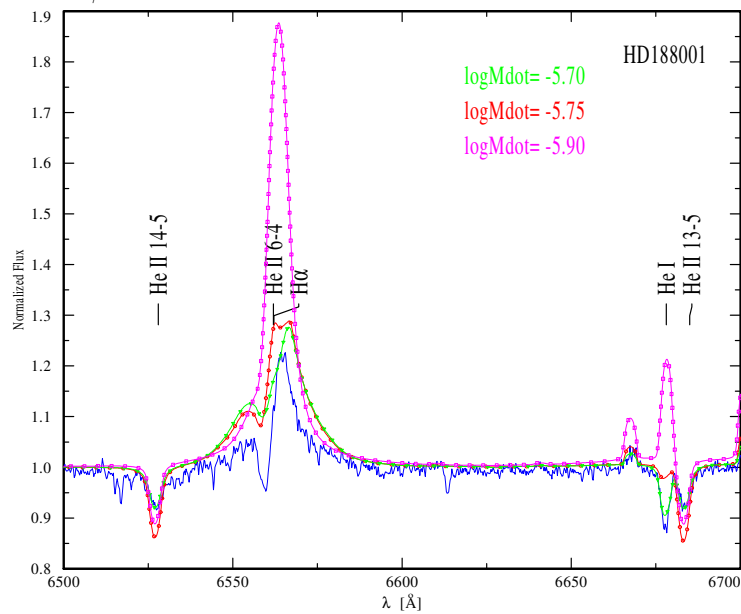
5.2.2   Mass-loss rate

Since for both stars values of mass-loss rates, which we adopted from literate (see Table 5.5), could not give satisfactory fit, particularly fit with H_α and P V lines, we decided to vary the value of $\dot{M}$. PoWR models with different values of mass-loss rates assuming microclumping with clumping factor D=10 were calculated. In Fig. 5.11a optical part of spectra and influence of $\dot{M}$ on line profiles is shown. As the value of $\dot{M}$ is increased the line profiles get more intense The finally adopted value of $\dot{M}$ is listed in Table 5.8. For the star HD 34656 the literature value of mass-loss was overestimated, while for the star HD 188001 the literature value of mass-loss was underestimated.

Problem that is present when deriving mass-loss rate from optical and UV diagnostics is discrepancy between values derived from fitting the H_α line and those obtained by fitting P V line and that the values derived from P V diagnostics give lower values than those derived by H_α diagnostics. Possible solution for this discrepancies is different treatment of clumping (see next section and paper by Šurlan et al. (2013)).

(a) Fits of H_β line for different values of mass-loss rate for HD 188001.

(b) Fits of H_α line for different values of mass-loss rate for HD 188001.

Figure 5.10: Line profiles of the H_α and H_β lines calculated with different value of He abudance for the star HD 188001.Blue full line represents the observation, while other lines represents line profiles calculated with PoWR for value od $\log \dot{M}$ of -5.70 (green line with triangle), -5.75 (red line with circles) and -5.90 (violet line with squares).
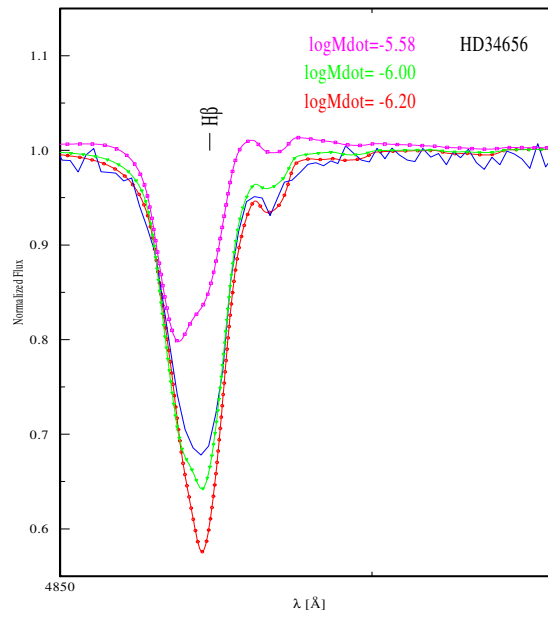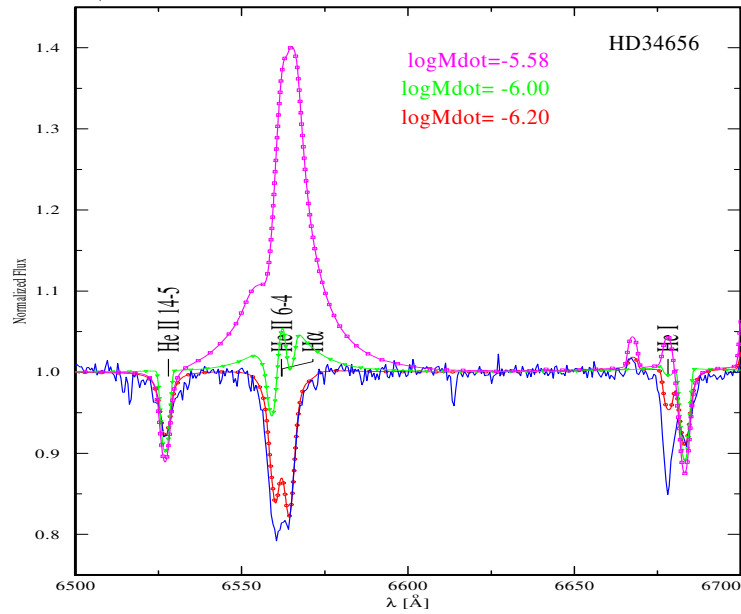
(a) Fits of H_β line for different values of mass-loss rate for HD 34656.

(b) Fits of H_α line for different values of mass-loss rate for HD 34656.

Figure 5.11: Line profiles of the H_α and H_β lines calculated with different value of He abudance for the star HD 34656.Blue full line represents the observation, while other lines represents line profiles calculated with PoWR for value od $\log \dot{M}$ of -5.58 (violet line with squares), -6.00 (green line with triangle) and -6.20 (red line with circles).

Table 5.6: Fixed model parameters used in the 3-D Monte-Carlo code.

| Model parameters	Value
Inner boundary of the wind	$r_{min} = 1\,R_*$
Outer boundary of the wind	$r_{max} = 100\,R_*$
Clump separation parameter*	$L_0 = 0.5$
Clumping factor	$D = 10$
Onset of clumping*	$r_{cl} = 1\,R_*$
Velocity at the photosphere	$v_{min} = 12\,[\mathrm{km\,s^{-1}}]$
Doppler velocity	$v_{dop} = 20\,[\mathrm{km\,s^{-1}}]$
Clumping parameter	$D = 10$

5.2.3   Clumping parameters

After the mass-loss rate was derived from fitting the H_α line profiles, the stratification of the P V ionization fraction and photospheric spectra were extracted from the final PoWR model and used as input for calculating the 3-D Monte-Carlo radiative transfer in the clumped wind as described in Section 3.4. Velocity of the wind is described by a double-β law (Hillier and Miller, 1999) with the same parameters used in PoWR for consistency. The clumping factor D and the Doppler-broadening velocity were taken the same as ones used in PoWR modeling. As was already described (see again Section 3.4) certain values of the clumping parameters were fixed, the interclumpmedium density factor d and the velocity deviation parameter m were varied in order to obtain the best fit to the observed P V doublet lines. Their final values are listed in Table 5.7. The P V resonance doublet as expected is being far too strong by the PoWR models for both stars (see red full lines in Figs. 5.12a and 5.12b). In contrast, very good agreement with observations is achieved with the 3-D Monte-Carlo simulations (see black dotted lines in Figs. 5.12a and 5.12b). The disagreement in the red component of the P V $\lambda\lambda 1118, 1128$ line of both stars is caused by blending with the Si IV $\lambda 1128$ line, which is not included in 3-D Monte-Carlo simulations.

Table 5.7: Clumping parameters which give the best fit to the observed P V line profiles. All other model parameters are given in Table 5.6.

Star	d	m
HD 34656	0.1	0. 01
HD 188001	0.01	0.001
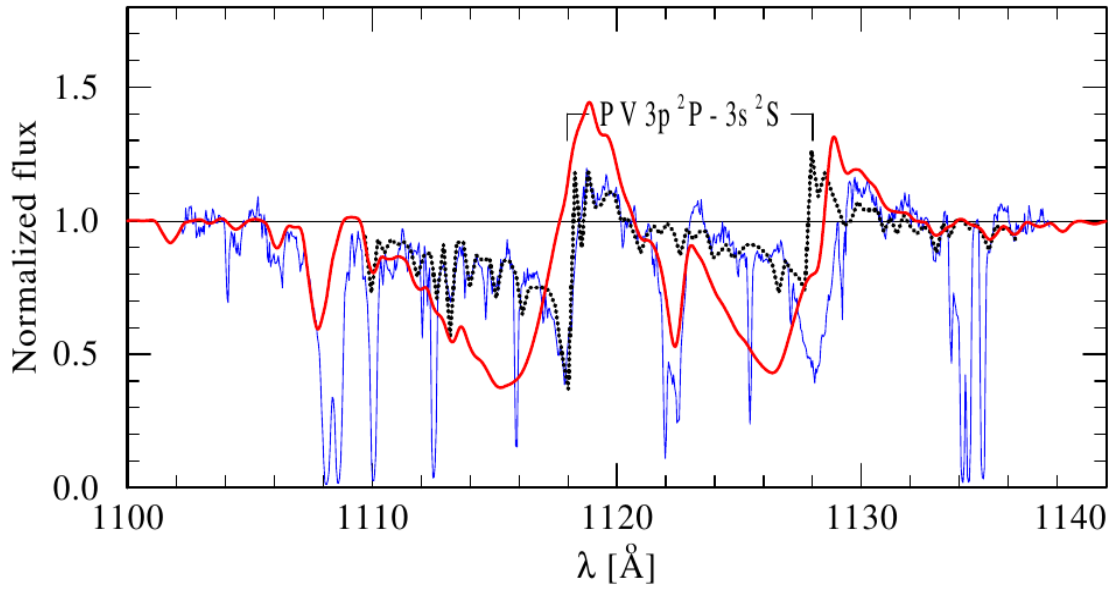
(a) Fits of P V doublet for different values of clumping parameters for HD 34656.
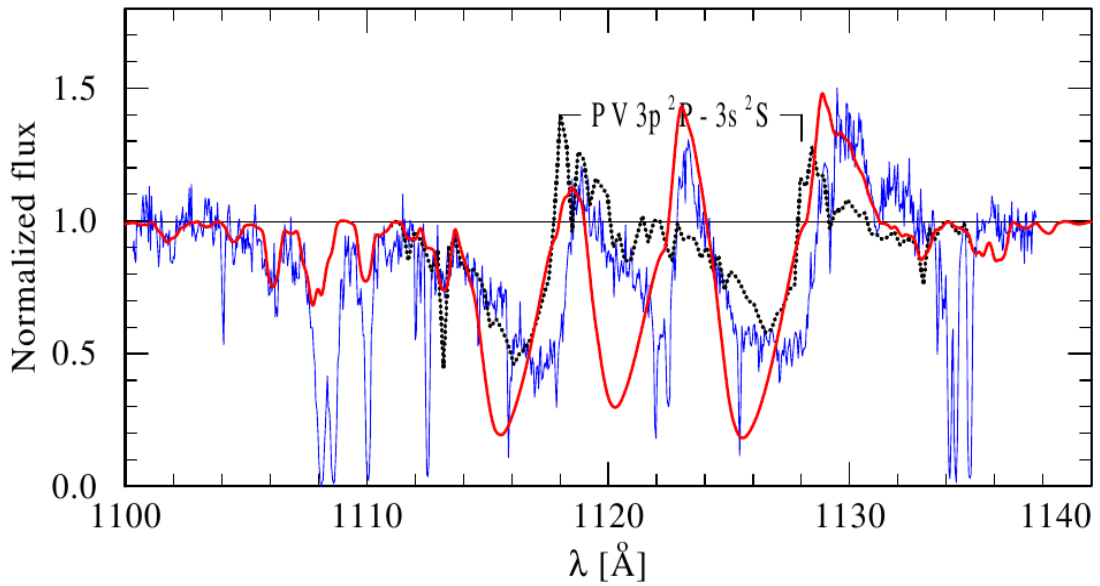
(b) Fits of P V doublet for different values of clumping parameters for HD 188001.

Figure 5.12: Line profiles of the P V doublet calculated with PoWR and 3-D Monte Carlo Radiative Transfer code for inhomogeneous winds.Blue full line represents the observation, while other lines represents line profiles calculated with PoWR (full red line) and with 3-D Monte Carlo Radiative Transfer for inhomogeneous winds (dotted black line).

Final stellar and wind parameters derived in this Thesis, using PoWR code, are summarised in the Table 5.8.

Table 5.8: Derived stellar and wind parameters

Parameter	HD 34656	HD 188001
T_{eff} (K)	33000	32500
$\log g$	3.50	3.35
E(B-V)	0.32	0.32
R_V	3.40	3.49
$\log \dot{M}(M_\odot \ yr^{-1})$	-6.20	-5.75
v_∞ (km s^{-1})	2150	1800
β	1.09	0.7

Chapter 6

Summary

In this thesis two Galactic O-type stars HD 34656 and HD 188001 were analyzed. Analysis was done in optical and UV spectral regions. Optical spectra were obtained by Perek 2-m telescope in Ondřejov, while UV spectra were obtain by IUE and FUSE satellites.

Primary focus of the thesis was to estimate wind parameters of analyzed stars i.e., to determine v_∞, $\dot{M}$ and clumping parameters. As initial values of stellar and wind parameters, which was used as an input to PoWR code, were adopted from literature (see Tab. 5.3 and 5.5). After the first models were calculated it was seen that they do not provide satisfactory fit to observed spectra and some of the adopted values of stellar and wind parameters had to be changed. By varying those parameters new set of stellar and wind parameters was derived using PoWR model atmosphere code. The final values of the stellar and wind parameters derived are given in Tab. 5.3. Best spectral fits obtained are given in Appendix A.

The mass-loss rates, which were derived from H_α diagnostic, were further used as an input to 3-D Monte Carlo Radiative Transfer code for inhomogeneous winds and for the first time clumping parameters of analyzed stars were derived. In this way, with same mass-loss rates and suitable clumping parameters, simultaneously fit of H_α and P V line profiles was obtained. In this way, known discrepancies in deriving value of mass-loss rate from H_α and P V line profiles where solved. Similar results can be find in Šurlan et al. (2013).

We found that with the same clumping parameter it is possible to fit stars with same type and luminosity class like star HD 34656 from this work and the star HD 192639 from paper of Šurlan et al. (2013). Similar results were expected for HD 188001 and it will be examined in further work.

Future outlook Hot massive stars are luminous objects which exibit continuous outflow of particles from their surface, i.e., stellar winds. This wind impacts on the evolution of the star and it's host galaxy. In order to better understand evolution of hot massive stars and "feedback" effects, it is crucial to obtain reliable estimates of basic parameters of these objects. Today, with advancments in technology and building modern ground-based observatories and satellites it is possible to study hot massive stars in multi wavelenght manner. Investigating stars in this way enables

us to constrain stellar and wind parameters, which can further be used to tackle the question of stellar evolution. Since mass-loss rate directly influeces evolution of a star, it must be determined with great precision. Using multi wavelenght observations of hot stars combined with modern state-of-the-art model atmosphere codes we can find values of mass-loss rate and investigate how different values of this parameter influence stellar evolution. However, question of the solution for so called "P V problem" is still unanswered completely. This is, also, one of the topics for future research in the field of hot massive stars and their parameters.
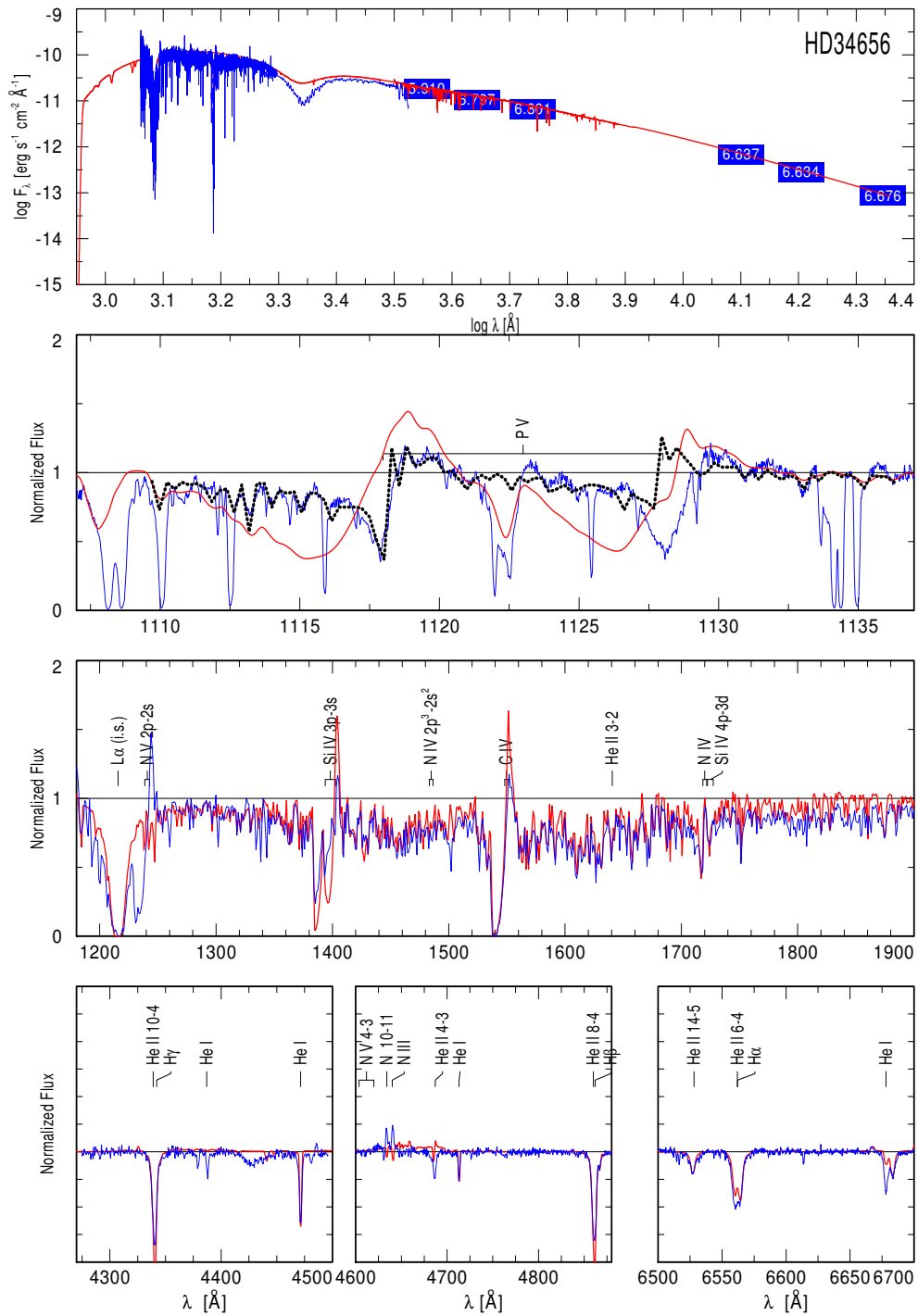
Appendix A

Spectral fits

Figure A.1: Best fit from PoWR modeling (thick red solid lines) to the observed HD 34656 spectra (thin blue solid lines), together with the calculated P V line profile from 3-D Monte-Carlo code (black dotted line). Blue labels with numbers in the upper panels are UBVJHK magnitudes.
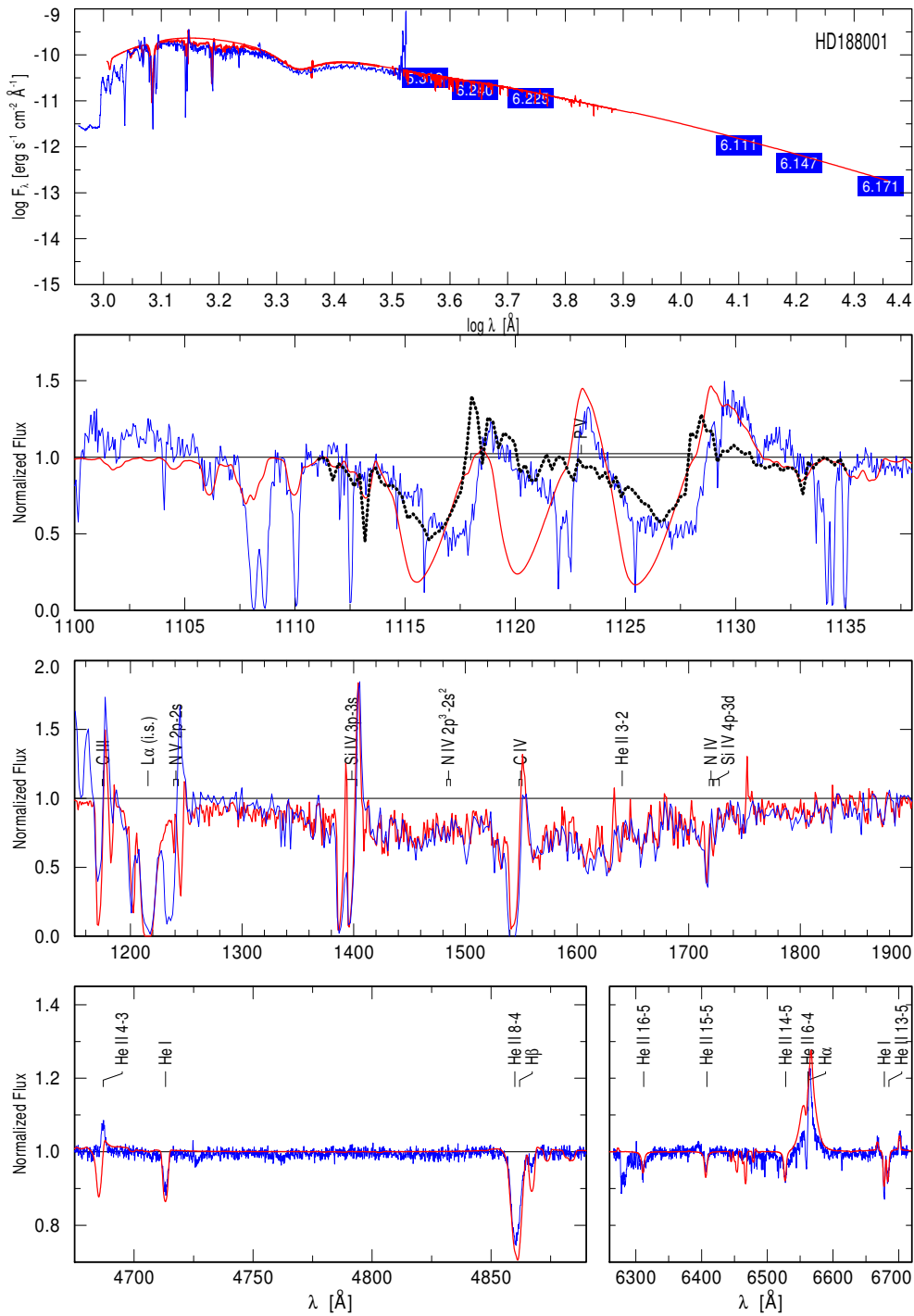
Figure A.2: Best fit from PoWR modeling (thick red solid lines) to the observed HD 188001 spectra (thin blue solid lines), together with the calculated P V line profile from 3-D Monte-Carlo code (black dotted line). Blue labels with numbers in the upper panels are UBVJHK magnitudes.
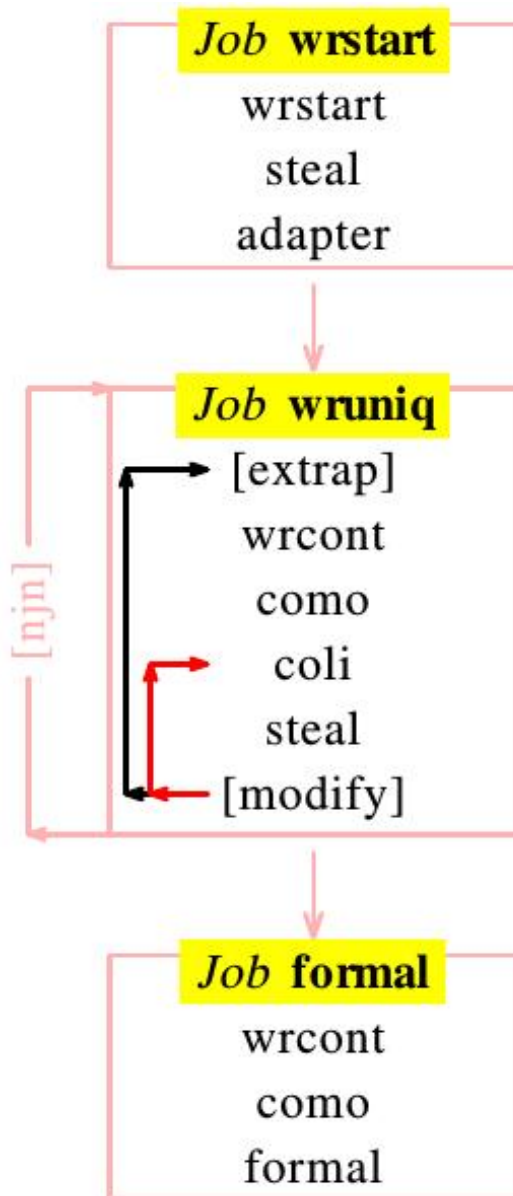
Appendix B

Flow of the PoWR code

Figure B.1: Flow of the PoWR code. Taken from http://www.astro.physik. uni-potsdam.de/~htodt/manpowr.pdf.

Bibliography

D. C. Abbott, J. H. Bieging, and E. Churchwell. Mass loss from very luminous OB stars and the Cygnus superbubble. *The Astrophysical Journal*, 250:645–659, Nov. 1981. doi: 10.1086/159412.

A. A. Aslanov and A. A. Barannikov. The possible nature of the periodic variability of the radial velocities and light of the runaway Of star HD 188001 (9 Sge). *Soviet Astronomy Letters*, 18:58, Feb. 1992.

A. A. Aslanov, L. N. Kornilova, and A. M. Cherepashchuk. A search for relativistic companions of runaway OB stars. *Pisma v Astronomicheskii Zhurnal*, 10:666–672, Oct. 1984.

M. Asplund, N. Grevesse, and A. J. Sauval. The Solar Chemical Composition. In T. G. Barnes, III and F. N. Bash, editors, *Cosmic Abundances as Records of Stellar Evolution and Nucleosynthesis*, volume 336 of *Astronomical Society of the Pacific Conference Series*, page 25, Sept. 2005.

J.-C. Bouret, D. J. Hillier, T. Lanz, and A. W. Fullerton. Properties of Galactic early-type O-supergiants. A combined FUV-UV and optical analysis. *Astronomy and Astrophysics*, 544:A67, Aug. 2012. doi: 10.1051/0004-6361/201118594.

J. A. Cardelli, G. C. Clayton, and J. S. Mathis. The relationship between infrared, optical, and ultraviolet extinction. *The Astrophysical Journal*, 345:245–256, Oct. 1989. doi: 10.1086/167900.

J. I. Castor, D. C. Abbott, and R. I. Klein. Radiation-driven winds in Of stars. *The Astrophysical Journal*, 195:157–174, Jan. 1975. doi: 10.1086/153315.

P. A. Crowther. Fundamental parameters of massive stars. *EAS Publications Series*, 13:1–20, 1 2004. doi: 10.1051/eas:2004048.

T. Eversberg, S. Lépine, and A. F. J. Moffat. Outmoving Clumps in the Wind of the Hot O Supergiant ζ Puppis. *The Astrophysical Journal*, 494:799–805, Feb. 1998. doi: 10.1086/305218.

A. Feldmeier. Time-dependent structure and energy transfer in hot star winds. *Astronomy and Astrophysics*, 299:523, July 1995.

A. W. Fullerton. Observations of Hot-Star Winds. In J. P. De Greve, R. Blomme, and H. Hensberge, editors, *Stellar Atmospheres: Theory and Observations*, volume 497 of *Lecture Notes in Physics, Berlin Springer Verlag*, page 187, 1997. doi: 10.1007/BFb0113486.

A. W. Fullerton, D. R. Gies, and C. T. Bolton. Detection of small-amplitude pulsations in HD 34656 (O7 II). *The Astrophysical Journall*, 368:L35–L38, Feb. 1991. doi: 10.1086/185942.

C. D. Garmany, P. S. Conti, and P. Massey. Spectroscopic studies of O type stars. IX - Binary frequency. *The Astrophysical Journal*, 242:1063–1076, Dec. 1980. doi: 10.1086/158537.

G. Gräfener, L. Koesterke, and W.-R. Hamann. Line-blanketed model atmospheres for WR stars. *Astronomy and Astrophysics*, 387:244–257, May 2002. doi: 10.1051/0004-6361:20020269.

W.-R. Hamann and G. Gräfener. Grids of model spectra for WN stars, ready for use. *Astronomy and Astrophysics*, 427:697–704, Nov. 2004. doi: 10.1051/0004-6361:20040506.

W.-R. Hamann, L. M. Oskinova, and A. Feldmeier. Spectrum formation in clumpy stellar winds. In W.-R. Hamann, A. Feldmeier, and L. M. Oskinova, editors, *Clumping in Hot-Star Winds*, page 75, Apr. 2008.

F. R. Harnden, Jr., G. Branduardi, P. Gorenstein, J. Grindlay, R. Rosner, K. Topka, M. Elvis, J. P. Pye, and G. S. Vaiana. Discovery of an X-ray star association in VI Cygni /Cyg OB2/. *Astrophysical Journal, Part 2 - Letters to the Editor*, 234:L51–L54, Nov. 1979. doi: 10.1086/183107.

A. Herrero, R. P. Kudritzki, J. M. Vilchez, D. Kunze, K. Butler, and S. Haser. Intrinsic parameters of galactic luminous OB stars. *Astronomy and Astrophysics*, 261:209–234, July 1992.

D. J. Hillier. Basic Parameters of Hot Massive Stars. In C. Leitherer, P. D. Bennett, P. W. Morris, and J. T. Van Loon, editors, *Hot and Cool: Bridging Gaps in Massive Star Evolution*, volume 425 of *Astronomical Society of the Pacific Conference Series*, page 113, June 2010.

D. J. Hillier and D. L. Miller. Constraints on the Evolution of Massive Stars through Spectral Analysis. I. The WC5 Star HD 165763. *The Astrophysical Journal*, 519:354–371, July 1999. doi: 10.1086/307339.

D. J. Hillier, T. Lanz, S. R. Heap, I. Hubeny, L. J. Smith, C. J. Evans, D. J. Lennon, and J. C. Bouret. A Tale of Two Stars: The Extreme O7 Iaf+ Supergiant AV 83 and the OC7.5 III((f)) star AV 69. *The Astrophysical Journal*, 588:1039–1063, May 2003. doi: 10.1086/374329.

D. J. Hillier, J.-C. Bouret, and F. Martins. Improving the Fundamental Accuracy of O-Star Parameters and Abundances. In L. Drissen, C. Robert, N. St-Louis, and A. F. J. Moffat, editors, *Proceedings of a Scientific Meeting in Honor of Anthony F. J. Moffat*, volume 465 of *Astronomical Society of the Pacific Conference Series*, page 237, Dec. 2012.

J. Krtička and J. Kubát. Radiatively Driven Winds of OB Stars – from Micro to Macro. In A. T. Okazaki, S. P. Owocki, and S. Stefl, editors, *Active OB-Stars: Laboratories for Stellare and Circumstellar Physics*, volume 361 of *Astronomical Society of the Pacific Conference Series*, page 153, Mar. 2007.

J. Krtička, J. Puls, and J. Kubát. The influence of clumping on predicted O star wind parameters. In W.-R. Hamann, A. Feldmeier, and L. M. Oskinova, editors, *Clumping in Hot-Star Winds*, page 111, Apr. 2008.

R. . Kudritzki and M. A. Urbaneja. Parameters and Winds of Hot Massive Stars. *ArXiv Astrophysics e-prints*, July 2006.

R.-P. Kudritzki and J. Puls. Winds from Hot Stars. *Annual Review of Astronomy and Astrophysics*, 38:613–666, 2000. doi: 10.1146/annurev.astro.38.1.613.

H. Lamers and J. Cassinelli. *Introduction to Stellar Winds*. Cambridge University Press, 1999. ISBN 9780521595650.

K. Lefever, J. Puls, and C. Aerts. A Grid of FASTWIND NLTE Model Atmospheres of Massive Stars. In C. Sterken, editor, *The Future of Photometric, Spectrophoto- metric and Polarimetric Standardization*, volume 364 of *Astronomical Society of the Pacific Conference Series*, page 545, Apr. 2007.

S. Lépine and A. F. J. Moffat. Direct Spectroscopic Observations of Clumping in O-Star Winds. *The Astronomical Journal*, 136:548–553, Aug. 2008. doi: 10.1088/ 0004-6256/136/2/548.

L. B. Lucy. The formation of resonance lines in locally nonmonotonic winds. *The Astrophysical Journal*, 255:278–285, Apr. 1982. doi: 10.1086/159826.

L. B. Lucy and P. M. Solomon. Mass Loss by Hot Stars. *The Astrophysical Journal*, 159:879, Mar. 1970. doi: 10.1086/150365.

J. Maiz-Apellaniz, N. R. Walborn, H. A. Galue, and L. H. Wei. VizieR Online Data Catalog: Galactic O star catalog (Maiz-apellaniz+, 2004). *VizieR Online Data Catalog*, 5116:0, Apr. 2004.

N. Markova, J. Puls, T. Repolust, and H. Markov. Bright OB stars in the Galaxy. I. Mass-loss and wind-momentum rates of O-type stars: A pure H\alpha analysis accounting for line-blanketing. *Astronomy and Astrophysics*, 413:693–709, Jan. 2004. doi: 10.1051/0004-6361:20031463.

F. Martins. Uv, optical and near-ir diagnostic of massive stars. *ArXiv Astrophysics e-prints*, 2010.

F. Martins. Empirical properties of very massive stars. *ArXiv Astrophysics e-prints*, 2014.

F. Martins, A. Hervé, J.-C. Bouret, W. Marcolino, G. A. Wade, C. Neiner, E. Alecian, J. Grunhut, and V. Petit. The MiMeS survey of magnetism in massive stars: CNO surface abundances of Galactic O stars. *Astronomy and Astrophysics*, 575:A34, Mar. 2015. doi: 10.1051/0004-6361/201425173.

M. V. McSwain, T. S. Boyajian, E. D. Grundstrom, and D. R. Gies. A Spectroscopic Study of Field and Runaway OB Stars. *The Astrophysical Journal*, 655:473–483, Jan. 2007. doi: 10.1086/509914.

D. Mihalas. *Stellar Atmospheres*. A Series of books in astronomy and astrophysics. W. H. Freeman, 1978. ISBN 9780716703594.

E. A. Milne. On the possibility of the emission of high-speed atoms from the sun and stars. *MNRAS*, 86:459–473, May 1926.

L. M. Oskinova, W.-R. Hamann, and A. Feldmeier. Neglecting the porosity of hot-star winds can lead to underestimating mass-loss rates. *Astronomy and Astrophysics*, 476:1331–1340, Dec. 2007. doi: 10.1051/0004-6361:20066377.

S. P. Owocki. Dynamical simulation of the "velocity-porosity" reduction in observed strength of stellar wind lines. In W.-R. Hamann, A. Feldmeier, and L. M. Oskinova, editors, *Clumping in Hot-Star Winds*, page 121, Apr. 2008.

S. P. Owocki, J. I. Castor, and G. B. Rybicki. Time-dependent models of radiatively driven stellar winds. I - Nonlinear evolution of instabilities for a pure absorption model. *The Astrophysical Journal*, 335:914–930, Dec. 1988. doi: 10.1086/166977.

J. Puls, R.-P. Kudritzki, A. Herrero, A. W. A. Pauldrach, S. M. Haser, D. J. Lennon, R. Gabler, S. A. Voels, J. M. Vilchez, S. Wachter, and A. Feldmeier. O-star mass-loss and wind momentum rates in the Galaxy and the Magellanic Clouds Observations and theoretical predictions. *Astronomy and Astrophysics*, 305:171, Jan. 1996.

J. Puls, N. Markova, S. Scuderi, C. Stanghellini, O. G. Taranova, A. W. Burnley, and I. D. Howarth. Bright OB stars in the Galaxy. III. Constraints on the radial stratification of the clumping factor in hot star winds from a combined H_α, IR and radio analysis. *Astronomy and Astrophysics*, 454:625–651, Aug. 2006. doi: 10.1051/0004-6361:20065073.

J. Puls, J. S. Vink, and F. Najarro. Mass loss from hot massive stars. *Astronomy and Astrophysicsr*, 16:209–325, Dec. 2008. doi: 10.1007/s00159-008-0015-8.

A. Sander, T. Shenar, R. Hainich, A. Gímenez-García, H. Todt, and W.-R. Hamann. On the consistent treatment of the quasi-hydrostatic layers in hot star atmospheres. *Astronomy and Astrophysics*, 577:A13, May 2015. doi: 10.1051/0004-6361/201425356.

F. D. Seward, W. R. Forman, R. Giacconi, R. E. Griffiths, F. R. Harnden, Jr., C. Jones, and J. P. Pye. X-rays from Eta Carinae and the surrounding nebula. *Astrophysical Journal, Part 2 - Letters to the Editor*, 234:L55–L58, Nov. 1979. doi: 10.1086/183108.

A. Slettebak. Of and Be stars. Introductory report. *Commmunications of the Konkoly Observatory Hungary*, 65:179–190, Jan. 1969.

A. Sota, J. Maíz Apellániz, N. R. Walborn, E. J. Alfaro, R. H. Barbá, N. I. Morrell, R. C. Gamen, and J. I. Arias. The Galactic O-Star Spectroscopic Survey. I. Classification System and Bright Northern Stars in the Blue-violet at R ˜ 2500. *The Astrophysical Journals*, 193:24, Apr. 2011. doi: 10.1088/0067-0049/193/2/24.

J. O. Sundquist, O. S. P., and P. J. The nature and consequence of clumping in hot, massive stars. *ArXiv Astrophysics e-prints*, 2011.

A. B. Underhill and J. M. Matthews. A Spectroscopic Orbit for the O8 If Star 9 SGE. *Publications of Astronomical Society of Pacific*, 107:513, June 1995. doi: 10.1086/133584.

B. Šurlan, W.-R. Hamann, J. Kubát, L. M. Oskinova, and A. Feldmeier. Three-dimensional radiative transfer in clumped hot star winds. I. Influence of clumping on the resonance line formation. *Astronomy and Astrophysics*, 541:A37, May 2012. doi: 10.1051/0004-6361/201118590.

B. Šurlan, W.-R. Hamann, A. Aret, J. Kubát, L. M. Oskinova, and A. F. Torres. Macroclumping as solution of the discrepancy between H_α and P v mass loss diagnostics for O-type stars. *Astronomy and Astrophysics*, 559:A130, Nov. 2013. doi: 10.1051/0004-6361/201322390.

J. S. Vink. Mass loss and the evolution of massive stars. *New Astronomy Reviews*, 52:419–422, Oct. 2008. doi: 10.1016/j.newar.2008.06.008.